Journal of *Marine Science and Engineering*

MDPI

*Review*

# $CO_2$ Capture and Sequestration by Gas Hydrates: An Overview of the Influence and Chemical Characterization of Natural Compounds and Sediments in Marine Environments

**Lorenzo Remia, Andrea Tombolini, Rita Giovannetti * and Marco Zannotti**

Chemistry Interdisciplinary Project (ChIP) Research Center, Chemistry Division, School of Science and Technology, University of Camerino, 62032 Camerino, Italy; lorenzo.remia@unicam.it (L.R.); andrea.tombolini@studenti.unicam.it (A.T.); marco.zannotti@unicam.it (M.Z.)

* Correspondence: rita.giovannetti@unicam.it

## Abstract

Due to the rising atmospheric carbon dioxide levels driven by human activity, extensive scientific efforts have been dedicated to developing methods aimed at reducing its concentration in the atmosphere. A novel approach involves using hydrates as a long-lasting reservoir of $CO_2$ sequestration. This review provides an initial overview of hydrate characteristics, their formation mechanisms, and the experimental techniques commonly employed for their characterization, including X-ray, Raman spectroscopy, cryoSEM, DSC, and molecular dynamic simulation. One of the main challenges in $CO_2$ sequestration via hydrates is the requirement of high pressures and low temperatures to stabilize $CO_2$ molecules within the hydrate crystalline cavities. However, deviations from classical temperature-pressure phase diagrams observed in natural and engineered environments can be explained by considering that hydrate stability and formation are primarily governed by chemical potentials, not just temperature and pressure. Activity, which reflects concentration and non-ideal interactions, greatly influences chemical potentials, emphasizing the importance of solution composition, salinity, and additives. In this context the role of promoters and inhibitors in facilitating or hindering hydrate formation is discussed. Furthermore, the review presents an overview of the impact of marine sediments and naturally occurring compounds on $CO_2$ hydrate formation, along with the sampling methodologies used in sediments to determine the composition of these natural compounds. Special attention is given to the effect and chemical characterization of dissolved organic matter (DOM) in marine aquatic environments. The focus is placed on the key roles of various natural occurring molecules, such as amino acids, protein derivatives, and humic substances, along with the analytical techniques employed for their chemical characterization, highlighting their central importance in the $CO_2$ gas hydrates formation.

**Keywords:** $CO_2$ gas hydrates; carbon capture and storage; promoters; inhibitors; marine environment



Academic Editors: Hailong Lu, Timothy S. Collett, Umberta Tinivella and Yinan Deng

Received: 8 August 2025
Revised: 16 September 2025
Accepted: 30 September 2025
Published: 3 October 2025

**Citation:** Remia, L.; Tombolini, A.; Giovannetti, R.; Zannotti, M. $CO_2$ Capture and Sequestration by Gas Hydrates: An Overview of the Influence and Chemical Characterization of Natural Compounds and Sediments in Marine Environments. *J. Mar. Sci. Eng.* **2025**, *13*, 1908. https://doi.org/10.3390/jmse13101908



## 1. Introduction

Since the onset of the first industrial revolution, atmospheric $CO_2$ levels have increased exponentially, driven by the continuous growth in energy demand. Prior to industrialization, the concentration of carbon dioxide was approximately 280 ppmv; by 2020, it had surpassed 400 ppmv and continues to rise, showing no signs of decline (Figure 1) [1]. According to the UN Intergovernmental Panel on Climate Change (IPCC), if no substantial

measures are taken, a temperature increase of 1.5 °C above pre-industrial levels could pose a severe threat to both the environment and human health [2]. As a response, many industries and nations have intensified efforts to achieve Net Zero Greenhouse Gas (GHG) emissions by 2050 [3–5]. Two main strategies are being involved to reduce atmospheric $CO_2$: one related to the adoption of renewable energy sources, while the other focuses on harnessing natural sinks for long-term storage of greenhouse gases, primarily through carbon capture and sequestration (CCS) technologies [5,6].

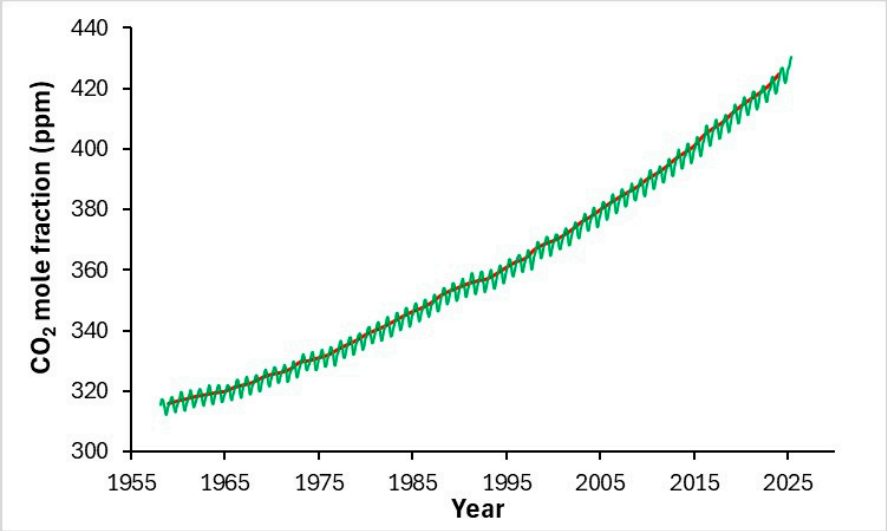


**Figure 1.** Graph reporting the increase in concentration of $CO_2$ in ppmv (NOAA Global Monitoring Laboratory); green line: monthly mean values; red line: monthly mean values corrected for the average seasonal cycle [7].

While renewable energy sources are now well established, CCS still faces challenges, particularly high costs, which require significant public and private investments to overcome [8].

Absorption and adsorption are the main techniques for $CO_2$ capture, with absorption being the most widely used. Absorption involves $CO_2$ dissolving in solvents, either physical by weak van der Waals forces (like Rectisol and Selexol) or chemical (mainly amines like 30% monoethanolamine, MEA). Chemical solvents are effective but require high energy for regeneration, causing about 65% of power plant energy use. Research continues on new solvents like amine blends, ionic liquids, and nanofluids to improve efficiency. Despite good performance, high costs and limited data restrict large-scale industrial use. Adsorption captures $CO_2$ by adhering it onto solid surfaces through physisorption or chemisorption, depending on the surface properties. Inorganic solid sorbents like activated carbon, zeolites, MOFs, silicates, polymers, and biochar are porous materials with large surface areas, where pore size and functionalization impact $CO_2$ capture capacity. Pressure increases generally enhance $CO_2$ loading. Current research aims to enhance the performance, cost-effectiveness, and scalability of adsorption systems by developing novel materials suitable for industrial $CO_2$ mitigation. In this context, a recent review discusses progresses in $CO_2$ capture technologies, focusing on the two main methods: absorption and adsorption [9].

Other sequestration techniques of common use are geological sequestration and mineral sequestration. Geological sequestration works similarly to what happens for the injection of hazardous wastes in subsurface; this technique, however, may cause leakage phenomena and thus the characteristics of the different rocks must be carefully determined prior to the process [10]. Also, in mineral sequestration, $CO_2$ is directly injected into soils and rocks; however, in this case, $CO_2$ is fixed as carbonate through mineralization,

which is facilitated by the presence of reactive rocks (such as mafic or ultramafic lithologies). The main advantage of this technique is the negligible risk of returning $CO_2$ to the atmosphere [11]. Less common CCS techniques are marine sequestration (or marine geological sequestration) and biological sequestration; the first method is analogous to the terrestrial geological sequestration; however, the direct injection of $CO_2$ can cause acidification of the surrounding seawater, leading to perturbation in the ecosystem [12]. Biological sequestration also finds little application due to the threat of possible loss of biodiversity; in addition to that carrying this process in marine ecosystem is not feasible, as it has low carbon capture capacity [13]. Lastly sequestration of $CO_2$ in hydrates represents a promising alternative, however research for this topic is still scarce, especially regarding large-scale applications [14–17]. Table 1 reports the aforementioned CCS methods, along with their advantages, disadvantages, and costs of operation (the costs of some techniques are not reported as they were not reported in any work).

The application of hydrates as reservoirs for atmospheric $CO_2$ is still under active investigation. Although hydrates were first discovered by Humphrey in 1810 and later synthesized by Faraday in 1820 [18], the earliest study of hydrates in marine environments dates back to 1934, when Hammerschmidt linked the blockage of oil and gas pipelines to the formation of $CH_4$ hydrates [19]. The first observation of $CO_2$ hydrates can be dated back to 1882, when Zygmunt Florenty Wróblewski [20], while studying carbonic acid, noted the formation of a white material resembling snow while raising the pressure. However, only recently the research on various aspects of hydrate formation has increased exponentially with numerous studies exploring the roles of both naturally occurring and synthetic molecules in promoting hydrate formation [21].

Owing to the greater thermodynamic stability of $CO_2$ hydrates compared to other typical industrial gas components such as nitrogen, hydrate-based processes have emerged as a promising approach for $CO_2$ capture. Additionally, the robust crystalline structure of gas hydrates enables the secure storage of large volumes of $CO_2$, making them a viable option for long-term sequestration in geological formations. Consequently, gas hydrates represent a potential technology for mitigating anthropogenic $CO_2$ emissions. Thus, gas hydrates can be suggested as a technology for mitigating $CO_2$ emissions [22].

Nowadays, research on gas hydrates, particularly $CO_2$ gas hydrates and their applications in carbon capture and storage (CCS), has been steadily increasing. This trend is illustrated in Figure 2, which displays the number of manuscripts published over the past 20 years (keywords "$CO_2$ hydrate" and "$CO_2$ clathrate" on the SCOPUS database).

With growing global interest in CCS, research into hydrate-based technologies is rapidly advancing. Several recent reviews have explored different aspects of $CO_2$ capture and sequestration using gas hydrates. These include, for example, the advantages of hydrate-based methods over conventional CCS technologies [23]; the state of the art in gas hydrate research with a focus on sustainable chemistry and industrial applications [24]; the chemistry of gas hydrates and their relevance to CCS, emphasizing carbon management and recent technological progress [22]; the potential of $CO_2$ hydrates as future cold energy storage materials and thermofluids [25]; and the current status of $CO_2$ replacement methods [26,27], etc.

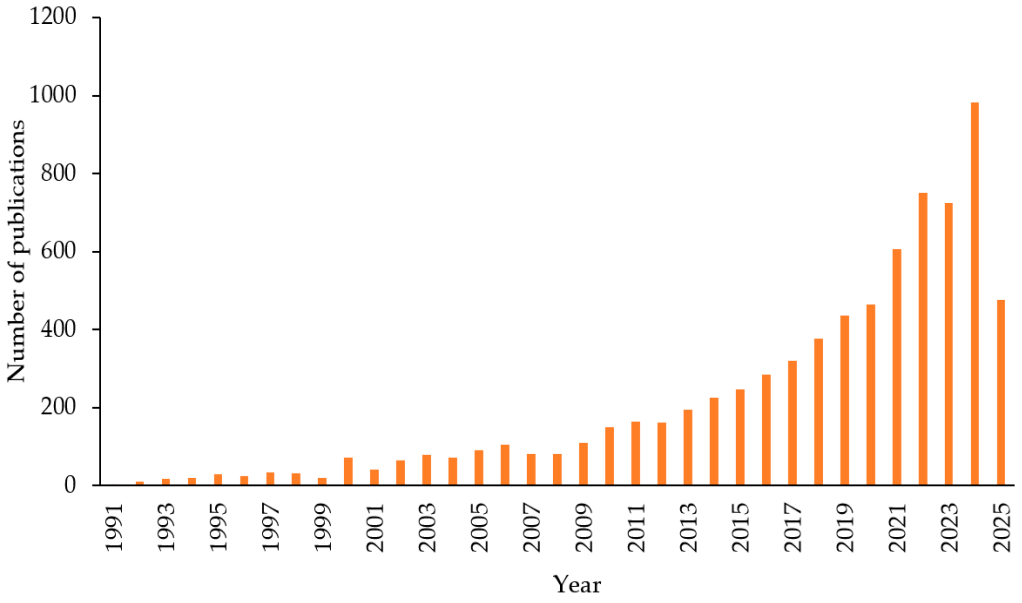


**Figure 2.** Results obtained from SCOPUS database using the keywords "$CO_2$ hydrate" and "$CO_2$ clathrate", the results of 2025 are reported as of June.

**Table 1.** Most common CCS methods present in the literature.

| Method | Advantages | Disadvantages | Cost |
|---|---|---|---|
| Solvent-based absorption (Propylene and amines) [28] | Most consolidated technique | Energy intensive, corrosion problems, solvent degradation and high maintenance cost [29] | between 40 and 100 USD/ton $CO_2$ [30] |
| Inorganic [31]<br>Polymeric Membrane [32–35]<br>Mixed matrix [36–40] | Better stability at different conditions of temperature, pressure and mechanical strain<br>Possibility to modulate physical properties like porosity<br>Easy and cost-effective synthesis<br>Both permeable and selective<br>Mechanical and thermal stability | Fragile and expensive<br>Not possible to Low stability (chemical and thermal) and plasticization tendency [41]<br>Need for the right proportions of fillers, to avoid lowering mechanical strength | 50 USD/$m^2$ of membrane [42,43]<br>USD/ton $CO_2$ depends on durability of the material<br>USD/ton $CO_2$ depends on durability of the material [28] |
| Geological sequestration [10] | Usage of depleted oil and gas reservoirs and coal seams | high leakage rate and inadequate capacity | Not determined yet |
| Biological Sequestration [13] | Nature-inspired process | Loss of biodiversity<br>In marine ecosystem CCS too low | |
| Mineral sequestration | Formation of stable carbonates [11] | Reactivity depends on the mineral composition [44] | |
| Ocean sequestration [12] | Direct injection from atmosphere | Ocean acidification and perturbation of ecosystems | |
| Storage in clathrates | Stable and with low leakage of $CO_2$ [27]<br>High storage capacity [45] | Still need research on formation and dissociation pathways | |

Following the current developments in the fields of $CO_2$ gas hydrates, unlike earlier reviews that focus narrowly on aspects such as formation kinetics or specific promoter classes in $CO_2$ hydrates, this review offers a broader and more integrated perspective. It begins with a general overview of $CO_2$ hydrate fundamentals and the most common

techniques used for their characterization. To investigate gas hydrates, various analytical techniques can be employed, including Raman spectroscopy, cryo-SEM, X-ray diffraction (XRD), and nuclear magnetic resonance (NMR). Additionally, preliminary insights are often gained through molecular dynamics simulations [46]. In addition, the effect of promoters and inhibitors are discussed, then key factors influencing hydrate formation in both laboratory and marine environments are explored. Special attention is given to natural compounds, such as dissolved organic matter, amino acids, protein derivatives, and humic substances, present in seawater, which can act as either promoters or inhibitors. The review also examines the role of sediments in the hydrate formation process and discusses sampling methodologies and analytical techniques used to characterize these natural compounds. By addressing both synthetic and naturally occurring influences, the review provides a comprehensive understanding of the variables affecting $CO_2$ hydrate formation.

## 2. Fundamentals of $CO_2$ Hydrates

### *2.1. Structural Characteristics of $CO_2$ Hydrates*

Gas hydrates are non-stoichiometric structures composed of water molecules connected by hydrogen bonds. Their cavities are large enough to encapsulate small gas molecules via van der Waals forces [47]. Three types of hydrate structures exist depending on formation conditions and guest molecule size: structure I (sI), structure II (sII), and structure H (sH) (see Figure 3). Structure I (sI) is the most common and can accommodate small molecules such as carbon dioxide, methane, ethane, and nitrogen (0.4–0.55 nm) [48], structure II (sII) hosts larger hydrocarbons (0.6–0.7 nm) as guest molecules [49] while structure H (sH) requires both large and small guest molecules, such as methane and cycloheptane, to remain stable [50].

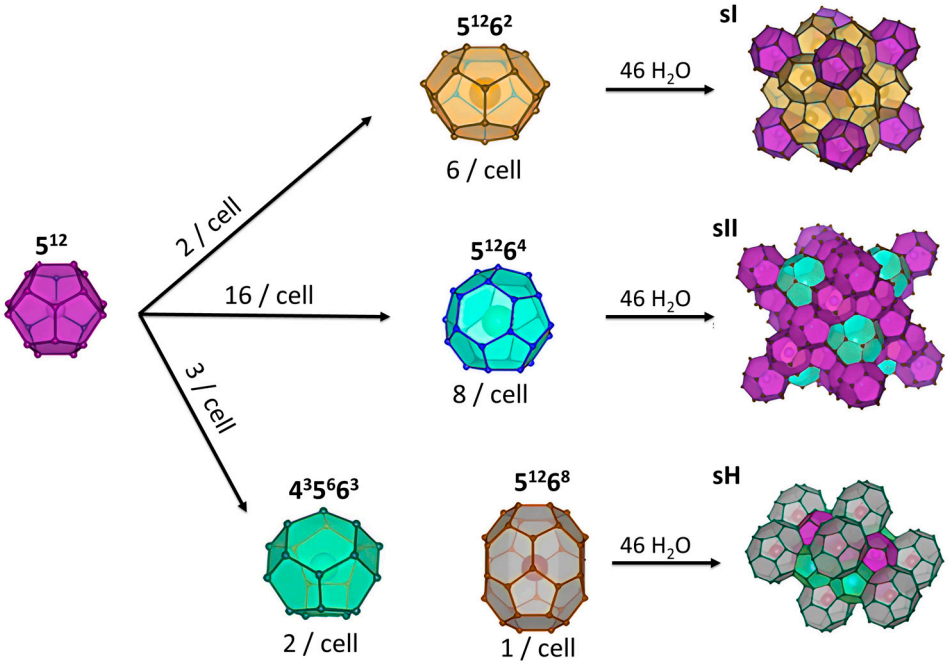


**Figure 3.** Schematic representation of the main structures of gas hydrates.

The sI structure contains 46 water molecules, arranged as two pentagonal dodecahedra ($5^{12}$) and six tetrakaidecahedra ($5^{12}6^2$). The sII structure, with 136 water molecules, is composed of alternating layers of 16 face-sharing pentagonal dodecahedra ($5^{12}$) and eight hexakaidecahedra ($5^{12}6^4$). The sH structure consists of 34 water molecules arranged as three pentagonal dodecahedra ($5^{12}$), two irregular dodecahedra ($4^35^66^3$), and one icosahedron ($5^{12}6^8$) (see Figure 3). Not all cavities in these polyhedra are the same size. The sI

structure has more large cavities compared to small ones, while sII contains mostly smaller cavities. The sH structure has an almost equal number of large and small cavities. The types of cavities and their average radii are detailed in Table 2. This distribution explains the different stability behaviors of the three structures regarding their ability to accommodate large and small guest molecules, as described earlier in this section [51,52].

**Table 2.** Parameter of cavities for different types of structures [51].

| **Structure** | **sI** | | **sII** | | **sH** | | |
|---|---|---|---|---|---|---|---|
| Cavity type | Small | Large | Small | Large | Small | Medium | Large |
| Number of cavities | 2 | 6 | 16 | 8 | 3 | 2 | 1 |
| Average cavity radius (Å) | 3.95 | 4.33 | 3.91 | 4.73 | 3.94 | 4.04 | 5.79 |
| Lattice dimension (Å) | 12 | | 17.3 | | 12.2 | | |
| Number of water molecules | 46 | | 136 | | 34 | | |

In particular, $CO_2$ hydrates are formed in structure sI, in which eight carbon dioxide molecules occupy pentagonal dodecahedral and tetrakaidecahedral cavities in a 1:3 ratio with only a few $CO_2$ molecules occupying small cages. However, it is difficult to differentiate which cavities are occupied when using Raman spectroscopy, since the spectrum shows only a single peak [52]. However, not every single cage is occupied by gas molecules, so a functional parameter is represented by the hydration number $n$ [53] (the molar ratio of water to gas molecules), defined by Equation (1):

$$n = \frac{N_w}{\sum_i N_i \theta_i} \quad (1)$$

where $N_w$ is the number of water molecules (46 for $CO_2$ hydrates), $\theta_i$ is the occupancy in i cages, and $N_i$ is the number of cages of the same kind.

### 2.2. Characterization of $CO_2$ Hydrates

In this section the most common methods used for the study of hydrates are reported:

Raman spectroscopy is an essential technique that provides insight into the formation and decomposition mechanisms of hydrates by analyzing their Raman spectra, which reflect molecular structures based on vibrational and rotational motions of molecules. In the case of hydrates, interactions between guest molecules and the water lattice affect the intensity, position, and number of spectral bands. When examining water, the most intense bands correspond to the symmetric and asymmetric OH stretching vibrations, located between 3000 and 4000 $cm^{-1}$. Variations in temperature, phase, chemical environment, and the nature of host molecules directly influence the intensity and position of these bands [54,55]. When $CO_2$ is encapsulated within the hydrate structure, two peaks can be observed in the 1200–1400 $cm^{-1}$ region of the Raman spectrum (as shown in Figure 4). These correspond to the C–O stretching vibration ($\nu_1$) and the overtone of the bending modes O–C–O ($2\nu_2$), known as the characteristic Fermi-diad peaks of $CO_2$ in hydrate structures [56]. The data obtained from Raman spectra, however, cannot be directly correlated to the quantity of $CO_2$ inside the hydrate structure; instead, it can be estimated from the ratio of the total area of the two $CO_2$ peaks to the area of the water peak [57]. In addition to that, Raman spectroscopy can also be used to monitor the replacement of $CO_2$ in hydrates by different guest molecules.

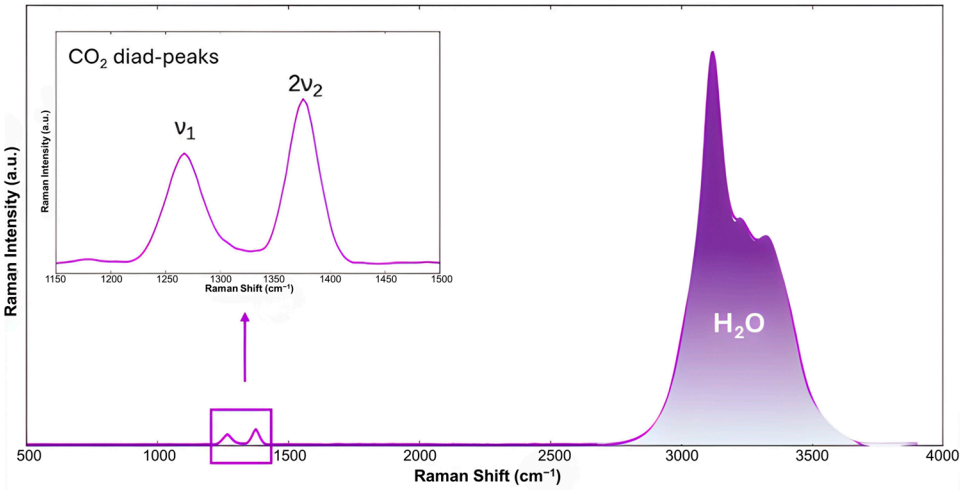


**Figure 4.** Raman spectra of $CO_2$ hydrate at 213 K showing the $CO_2$ Fermi-diad peaks and OH stretching bands of water, adapted from [58].

Cryo-SEM provides valuable information about the morphology of hydrates and the shape of their pores. This is crucial for understanding the physical and morphological properties of gas hydrates. The technique requires refrigeration below −30 °C because the hydrate structure of water is lost if the analysis is performed at room temperature. For example, Figure 5 shows two SEM images of a $CO_2$ hydrate, as reported by Giovannetti et al. [58]. These are present as spherules with dimensions on the order of tens of micrometers, formed by $CO_2$ diffusion during hydrate formation. At higher magnification of the sample (Figure 5b), cavities can be observed containing holes. This is likely due to the loss of $CO_2$ from the cavities, possibly favored by the interaction with the electron beam of the microscope. This technique can also be used to study the "self-preservation" of $CO_2$ hydrates as reported by Falenty et al. [59] that used cryo-SEM, in combination with in situ neutron diffraction; in this phenomenon hydrates show a slow decomposition even outside of their stability range, successfully correlating the "self-preservation" to the permeability of the ice film formed during the decay of the gas hydrate surface.

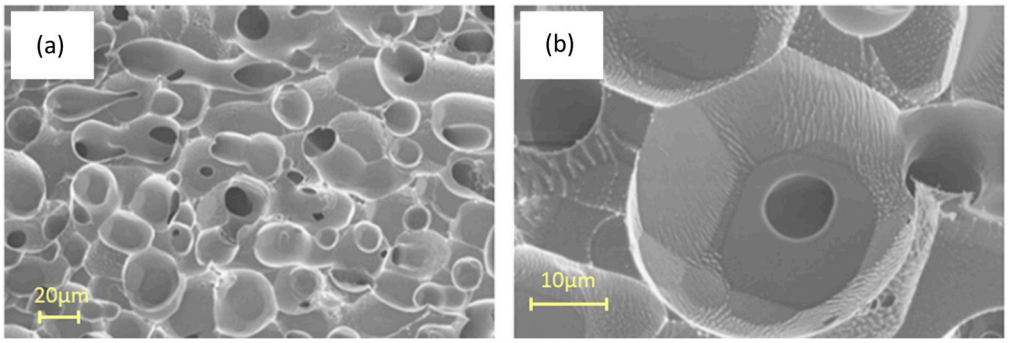


**Figure 5.** (**a**) SEM images showing the surface morphology of $CO_2$ hydrates; (**b**) hydrate structure at an higher magnification, adapted from [58].

Powder X-ray diffraction (pXRD) is another technique used to determine the structure and composition of $CO_2$ hydrates, including the location of guest molecules and cage occupancies [60]. As with other analytical methods, XRD measurements on hydrates must be performed under low temperature and high-pressure conditions to prevent hydrate decomposition. One of the main advantages of XRD is its ability to distinguish ice from hydrate, as well as to measure the rates of hydrate formation and decomposition directly

in situ. This is typically achieved by calculating the intensity ratio of the diffraction peaks corresponding to the hydrate phase [61].

NMR is one of the most common magnetic resonance techniques used for the analysis of gas hydrates. The primary methods include NMR spectroscopy and MRI (magnetic resonance imaging), which are typically employed to evaluate the presence of specific components and their saturations with minimal influence from experimental conditions such as temperature and pressure [62]. $^{1}H$ and $^{13}C$ NMR spectroscopy are used to study crystal structures and cage occupancies of guest molecules or how $CO_2$-encased molecules reorientate in the hydrate structure. Ratcliffe et al. [63] highlight the importance of temperature-dependent dynamics in interpreting NMR data for $CO_2$ hydrates. The study proposes several motional models, including libration in one or two planes, to explain the observed NMR spectra. In particular, the $^{13}C$ NMR line shapes change with temperature, reflecting different motional regimes. Furthermore, MRI provides information on gas hydrate formation and dissociation in porous media, as well as the replacement of guest molecules in the hydrate structure [64]; that being said, some recent studies also used NMR for quantitative analysis of the formation and dissociation of $CO_2$ hydrates [65,66]. Additionally, some studies have utilized NMR to investigate the replacement of methane by $CO_2$ [67].

Differential Scanning Calorimetry (DSC) is a thermal analysis technique used to study the thermodynamic properties of hydrates. DSC measures the difference in heat flow between a sample and a reference during a controlled temperature program, providing information about phase transitions and allowing prediction of hydrate stability under specific conditions [68]. Additionally, DSC is employed to quantify the amounts of hydrate, unreacted ice, and unreacted guest molecules [69]. Figure 6 shows an example of a heat flow chart reported by Lee et al. [70], where the distinct heat flow changes corresponding to different types of phase transitions can be clearly observed.

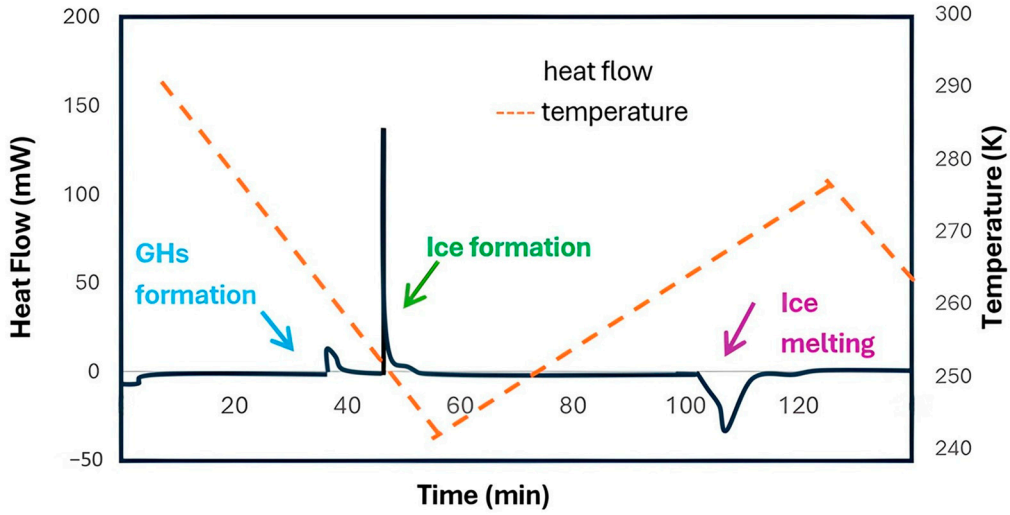


**Figure 6.** DSC analysis of a $CO_2$ hydrate sample; adapted from [70].

Computational approaches can be used to predict the behavior of hydrates, especially during preliminary studies. Molecular Dynamics (MD) simulations, in particular, offer valuable insights into the formation–decomposition mechanisms and stability of hydrates. The first MD simulations on hydrate growth can be dated back to the 1980s [71,72]; since then, researchers have applied these simulations to evaluate various factors influencing hydrate formation and dissociation. Figure 7 presents the most common MD models applied to study $CO_2$ hydrates, as collected by Zhang et al. [73].

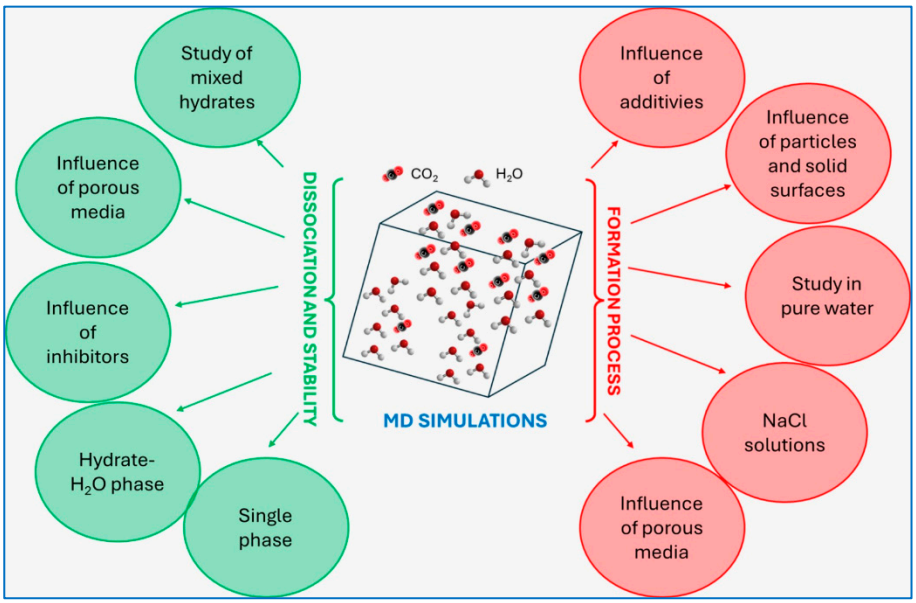


**Figure 7.** Diagram reporting different MD models applied to the study of $CO_2$ hydrates [73].

### *2.3. Thermodynamic and Kinetic Aspects*

#### 2.3.1. Thermodynamic Aspects

Thanks to advances in experimental and computational techniques, it is possible to observe the various mechanisms involved in the formation of $CO_2$ hydrates. The thermodynamic properties of $CO_2$ hydrates provide valuable information about their formation, decomposition, and stability [74]. To identify the factors influencing $CO_2$ hydrate formation, a proper understanding of the hydrate phase equilibrium is essential.

Most thermodynamic research relies on computational simulations. In recent years, the focus has shifted towards mixed $CO_2$ hydrate systems as opposed to pure $CO_2$ hydrates, resulting in a relatively limited amount of the literature available on the latter to date [16].

Usually, phase equilibrium is calculated by considering the system as composed of two liquid phases separated by a thin hydrate layer. The hydrate–liquid water (H-Lw) equilibrium is modeled based on the hydrate–water–$CO_2$ system [75].

Figure 8 displays a representative phase diagram of the $H_2O$–$CO_2$ system, illustrating the phase transitions of water and $CO_2$ within the mixed system. The area shaded in gray corresponds to the stability zone of $CO_2$ hydrates when carbon dioxide is introduced in its gaseous state. As will be discussed in the following chapters, it is important to note that the temperature and pressure conditions governing hydrate stability can shift depending on several factors, such as the nature of the additives employed and the characteristics of the sediments in which the hydrates are formed.

From a thermodynamic perspective, the first law of thermodynamics ensures energy conservation during hydrate formation, while the second law governs the direction of processes, favoring spontaneous transformations that minimize Gibbs free energy (G). When a system can reach thermodynamic equilibrium, the equilibrium conditions are defined by this energy minimization across temperature, pressure, and component mass distribution.

However, if thermodynamic equilibrium is not attainable, as is often the case in complex natural environments, the system evolves according to the combined law, which dictates alternative paths for development toward lower energy states. Under these circumstances, hydrate phase stability curves, such as those in Figure 8, represent only possible boundaries, and may not reflect the actual phase behavior. Competing transitions or mass

conservation constraints may result in more favorable thermodynamic outcomes, such as alternative hydrate structures or dissolution dynamics.

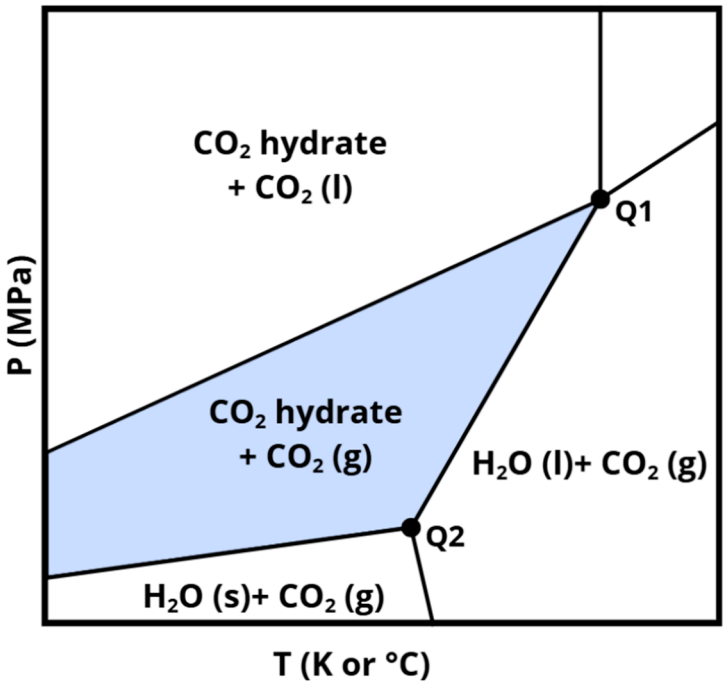


**Figure 8.** Pressure-temperature phase diagram of a $CO_2$–$H_2O$ system.

A rigorous thermodynamic analysis must account not only for temperature (T) and pressure (P), but also for the chemical potentials of the guest molecules and water in both the hydrate and surrounding phases. The stability of gas hydrates is fundamentally governed by the equality of chemical potentials rather than by T and P alone. Specifically, hydrate formation and stability result from the chemical potentials of both the guest molecule (e.g., $CO_2$, $CH_4$) and water in the hydrate and in the adjacent phases such as aqueous solution, gas phase, or other host environments [76].

Chemical potentials depend on species' activities, not merely concentrations (mole fractions) or partial pressures. In aqueous or mixed phases, activity reflects interaction effects such as non-ideal solution behavior, salinity influences, presence of additives (e.g., salts, inhibitors, promoters), or geological matrix effects. For gases like $CO_2$ or $CH_4$ dissolved in water, Henry's law constants and activity coefficients modulate the activities, influencing chemical potential; water activity itself can be altered by dissolved salts or organic compounds. Thus, concentration effects in all phases influence the chemical potentials and, ultimately, the hydrates' stability. This explains why identical T-P conditions can support or inhibit hydrate formation depending on phase composition [76,77].

In this contest, chemical potentials are essential; in fact, classical hydrate phase diagrams plot only equilibrium based on partial pressure of gas and temperature, implicitly assuming ideal behavior and fixed composition. Natural systems (marine sediments, pipelines, porous media) exhibit complex multi-component mixtures, gradients, and therefore non-idealities. In addition, transport phenomena (mass transfer limitations), presence of multiple phases (e.g., gas pockets, saline pore water), and mineral interfaces create heterogeneous chemical potential fields. Hence, chemical potential equality is the true thermodynamic criterion for hydrate stability, while T and P are necessary but insufficient descriptors [78].

Equilibrium conditions for hydrate formation or dissociation are established when the chemical potential of the "building unit" (typically, guest molecule plus n($H_2O$)) in

solution equals that within the hydrate phase. The driving force for hydrate growth or decomposition is the difference in chemical potential ($\Delta\mu$) between the surrounding phase and the hydrate phase, which can be expressed as (i) $\Delta\mu > 0$: hydrate growth or nucleation occurs; (ii) $\Delta\mu = 0$: phase equilibrium is established; (iii) $\Delta\mu < 0$: hydrate decomposition occurs [79].

Concentrations, reflected in the activities, and therefore in the chemical potentials, of guest and water molecules in all coexisting phases, are crucial to determine the system equilibrium. Hence, considering only temperature and pressure is insufficient; the gas composition, degree of saturation in water (or other host phases), and the presence of solutes or additives significantly affect chemical potentials and thus stability [80].

This issue can be evaluated by considering the system's degrees of freedom, using a compressed form of the Gibbs phase rule: [F = C − P + 2] where F is the number of degrees of freedom, C is the number of components, and P the number of phases. For example, in a system forming $CH_4$ hydrate with methane, water, and hydrate phases (C = 2, P = 3), the system has F = 1, allowing one independent variable (temperature or pressure) to be adjusted during equilibrium measurements [77].

Nevertheless, in natural settings, both temperature and pressure vary locally, and more than one hydrate phase may be present, along with minor but thermodynamically influential phases like adsorbed water layers, gas–liquid interfaces, and mineral surfaces. In such cases, the system becomes mathematically overdetermined, and equilibrium modeling must give way to non-equilibrium thermodynamic analysis. This explains why actual hydrate formation and dissociation may diverge from theoretical models [78].

Even though microscale numerical simulations have managed in calculating interactions between gas molecules and water cages, their reliability strongly depends on the accuracy of the interaction potential energies and the models employed [16]. In real marine environments, the complexity and variability of conditions, such as temperature, pressure, salinity, and geological heterogeneity, significantly influence these parameters, making precise prediction of $CO_2$ hydrate behavior challenging. Experimental and simulation studies have also demonstrated deviations from classical trends—for example, although higher pressures and lower temperatures generally enhance hydrate growth, exceptions underline the need for further refinement of existing models. Some experimental approaches are possible; for example, Yang et al. [81] measured the $CO_2$ solubility in H–Lw equilibria using an experimental apparatus and found a good agreement with the theoretical results for the same system. Additionally, DSC is used to determine the values of enthalpy of dissociation and heat capacity values of $CO_2$ hydrate systems.

#### 2.3.2. Kinetic Aspects

The formation kinetics of gas hydrates are governed by a complex interplay of thermodynamic and dynamic factors, including temperature, pressure, gas composition, and the presence of nucleation sites such as interfaces or solid surfaces [82].

While classical thermodynamic models provide a framework for predicting hydrate stability, experimental observations frequently reveal deviations from these predictions, indicating the presence of kinetic anomalies.

A particularly illustrative example is found in mixed gas systems containing $CO_2$ and methane $CH_4$. Thermodynamically, $CO_2$ forms more stable hydrate structures than $CH_4$ under comparable conditions. However, experimental studies have shown that $CH_4$ can initiate hydrate nucleation preferentially, even in the presence of $CO_2$. This behavior suggests that kinetic factors may override thermodynamic stability in determining the onset of hydrate formation [83].

Several hypotheses have been proposed to explain this phenomenon: (i) molecular diffusivity: $CH_4$ exhibits higher diffusivity in aqueous media compared to $CO_2$, potentially allowing it to reach nucleation sites more rapidly [84]; (ii) hydrate cage formation dynamics: $CH_4$ may more readily form metastable hydrate-like clusters that serve as precursors to full hydrate structures [76]; (iii) surface affinity: $CH_4$ may interact more favorably with available surfaces or interfaces, enhancing its nucleation potential [85]; (iv) competitive adsorption and incorporation: in mixed gas environments, $CH_4$ may dominate the initial stages of hydrate formation due to its kinetic accessibility, despite its lower thermodynamic driving force [86]. These findings have significant implications for the modeling and optimization of hydrate-based technologies, including carbon capture and storage (CCS), gas separation, and the exploitation of natural hydrate reservoirs. A deeper understanding of kinetic behavior is essential for accurately predicting hydrate formation pathways and designing efficient systems for industrial and environmental applications.

The hydrate formation process occurs in two stages: nucleation by creation of microscopic clusters and growth with rapid crystal expansion once nuclei exceed a critical size. Growth mechanisms vary depending on whether nucleation occurs in bulk phase (homogeneous) or at surfaces/pores (heterogeneous). Nucleation can be homogeneous, rare in real conditions or more commonly heterogeneous, which depends on surfaces or impurities to reduce the energy barrier. Several models have been developed: Labile Cluster Hypothesis [76], stochastic cluster collisions lead to nuclei. Local Structuring Theory [79], locally ordered water–gas zones evolve into hydrate structures. Blob Hypothesis [80] combines both theories. A key concept is that hydrate formation must overcome a Gibbs free energy barrier. The critical nucleus size (typically 2–4 nm) marks the transition beyond which growth becomes thermodynamically favorable. For $CO_2$, this barrier is higher than for $CH_4$, leading to longer induction times (delay before detectable hydrate formation), higher chance of nuclei dissociation before growth. This delay is especially relevant in $CH_4$–$CO_2$ replacement processes, where the reformation of methane hydrates during early stages can reduce efficiency [87].

Kinetic study can be approached in different ways to obtain both macrokinetics and microkinetics information [16].

The macrokinetic approach focuses on the overall steps involved in hydrate formation, which are similar for both mixed and pure $CO_2$ hydrates. The initial phase, which goes from the start of the reaction to the formation of critical nuclei, is called the induction time. During this period, nuclei are stabilized by hydrogen bonds formed between water molecules. Furthermore, induction time can be subdivided into microscopic induction time (ending with the formation of the first nuclei) and macroscopic induction time (ending when the first visible hydrate clusters appear), as illustrated in Figure 9 [88].

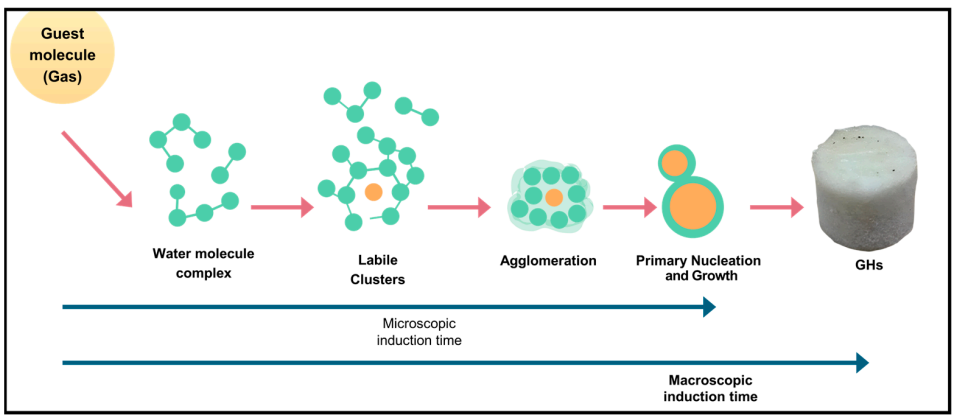


**Figure 9.** Schematic diagram illustrating the process of gas hydrate formation [88].

After the formation of critical nuclei, these nuclei begin to grow into larger and more stable clusters. This growth phase is typically accompanied by a pressure decrease [89], as illustrated in Figure 10. Factors influencing the induction time and growth rate of $CO_2$ hydrates include pressure, temperature, stirring rate, and reaction vessel size, with pressure and temperature being the most fundamental thermal parameters. Additionally, due to the limited contact area between gaseous $CO_2$ and the liquid phase, the use of porous media [90] or stirring [91,92] can enhance mass transfer and thus promote hydrate formation.

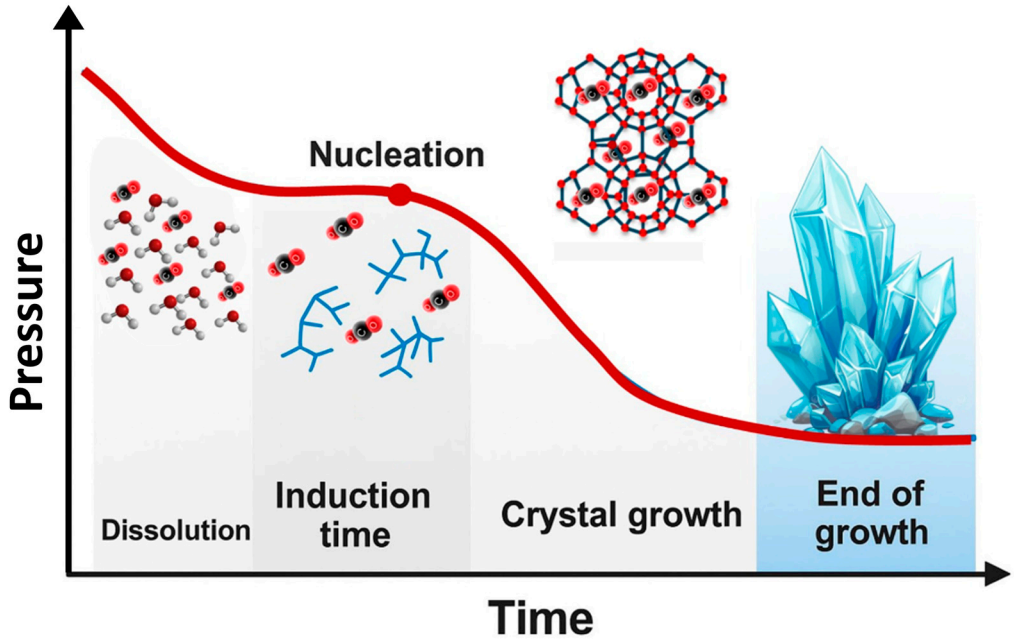


**Figure 10.** Graph showing pressure changes during the various stages of hydrate growth adapted from [82].

Microkinetics, on the other hand, focuses on studying the interactions between water cages and guest molecules through MD simulations, often incorporating quantum mechanical methods such as semiempirical orbitals and Density Functional Theory (DFT), which is based on the Schrödinger equation. This approach involves analyzing water–water and $CO_2$–water interaction potential energies [16] as well as employing ab initio techniques. Among these methods, DFT is the most widely used, as it enables determination of hydrate structure and identification of the cage occupancies of $CO_2$ molecules that are thermodynamically most stable [93]. Evaluating cage occupancies and guest molecule interactions within the hydrate structure is essential to predict structural stability and provides insights into the formation and dissociation mechanisms of $CO_2$ hydrates through detailed analysis of water arrangements [94]. These methods, however, give results based on single cages and, as such, do not consider the periodic environment of the hydrate lattice [95].

## 3. Promoters and Inhibitors

### *3.1. Promoters of $CO_2$ Hydrate Formation*

Hydrate nucleation depends on several factors, including undercooling, pressure, gas-to-water ratio, presence and concentration of promoters, agitation, and the type of gas. Promoters can be classified as thermodynamic (THP) and kinetic (KHP).

THPs favor hydrate formation at lower pressures and higher temperatures by facilitating the organization of the hydrate structures, with the promoters remaining trapped inside the hydrate cavities. If THPs promoters are present at less than the stoichiometric

concentration, they fill the large cages favoring the formation of structure II as schematized in Figure 11a that illustrates the difference in structure between pure $CO_2$ hydrate and binary THF + $CO_2$ hydrate. This phenomenon is called "tuning phenomenon" [96].

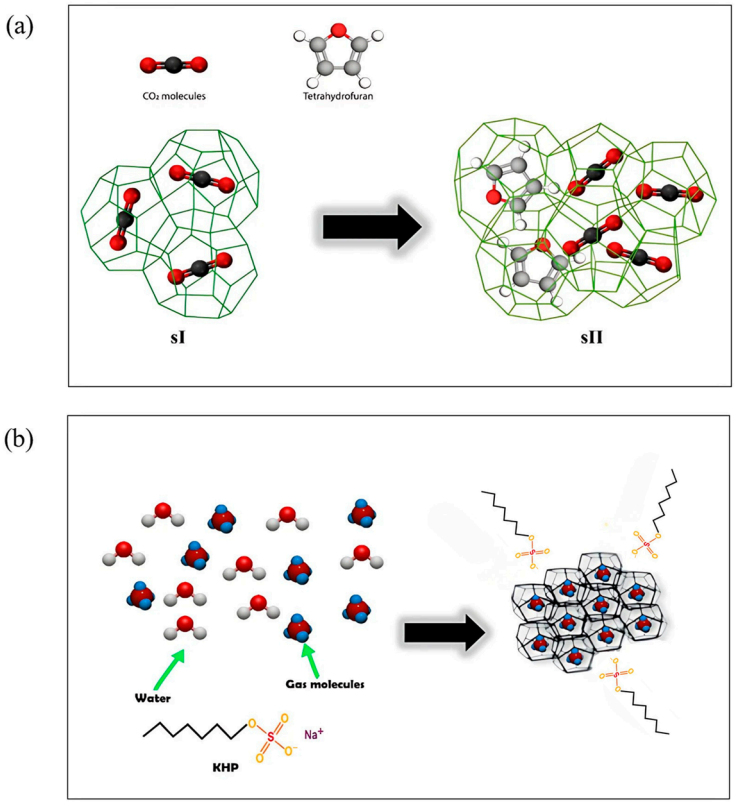


**Figure 11.** (**a**) Schematic diagram illustrating the effect of THP on the transition from pure $CO_2$ hydrate (sI) to THF + $CO_2$ hydrate (sII), adapted from [96]. (**b**) Mechanism of gas hydrate formation in presence of KHP, adapted from [97].

In addition, KHPs modify the interfacial tension and increase the surface area, enhancing the solubility of gases in water. This improves gas consumption and permeation rate during hydrate formation. Due to their molecular characteristics, KHPs do not enter the hydrate cages and thus do not affect the hydrate equilibrium curve of the hydrate (Figure 11b) [97]. While THPs therefore stabilize the structure, KHPs accelerate hydrate formation by shortening the induction time, without influencing structural transitions [98].

#### 3.1.1. Role of Surfactants and Additives

The first and most used class of KHPs for $CO_2$ hydrates is represented by surfactants, which have been employed since 1985, initially to improve heat storage capacity [99]. Even the addition of small amounts of surfactants significantly increases the rate of hydrate formation and, for certain surfactants, the need for stirring can be eliminated [100]. As previously noted, THPs therefore stabilize the hydrate structure, whereas KHPs enhance the hydrate formation rate by shortening the induction time, without affecting structural transitions [101,102].

The surfactant with the greatest impact on the kinetics of hydrate formation is sodium dodecyl sulfate (SDS), making it the most used promoter for this purpose [103].

It is, in fact, known that, even at low concentration, SDS can act as a good promoter for hydrate formation; however, when the concentration is increased drastically, a reduction in the $CO_2$ capture capacity is observed [104]. In addition, the efficiency of promotion was also observed to depend on the form in which SDS is used; Wang et al. [105] found that,

when adding SDS as micelle, a reduction in the formation rate of hydrates was observed. In general, the effect of a particular surfactant on hydrate formation mainly depends on its nature; considering the ionic properties, various studies related to the application of ionic surfactants (SDS, for example) reported a higher hydrate formation rate [106–108].

Another parameter to consider is the length of the surfactant's hydrophobic chain; therefore, different studies have been conducted using various surfactants with the same functional group but different chain length. In this case, it was observed that the presence of a longer chain favors the nucleation of hydrates, but the effect on the subsequent formation is heavily dependent on the type of hydrate [109–112]. It is important to note that only surfactants containing 12 carbon atoms are effective in promoting hydrate formation with pure $CO_2$, whereas for $CH_4$ and mixed hydrates, formation is also favored by the presence of surfactants with chain length from 8 to 14 [113].

The second most common additive used as THPs is tetrahydrofuran (THF). A particular effect of THF relates to its ability to change the $CO_2$ hydrate structure from sI to sII which results in higher $CO_2$ absorption [114]. As with many other promoters, this effect persists only up to a specific concentration; for THF, a plateau was observed at concentration above 5.56 mol%. What happens is that, as the THF concentration increases, the molecules will occupy sII cavities, thus reducing $CO_2$ storing capacity in the hydrate structure [115].

Other additives commonly used for hydrates formation include cyclopentane, 1,3-dioxalane [116], pyrrolidine, and aziridine [117]; all these compounds showed a promotional effect on $CO_2$ hydrate formation but a lower rate than SDS and THF. A particular case can be mentioned for 2-methyl tetrahydrofuran, which showed no effect on hydrate formation [116]. A novel field of study, mainly focused on promoting methane hydrate formation, is the application of multi-chain surfactants, also called Gemini surfactants, thanks to their better surface activity compared to single chain surfactants [118]. Gemini surfactants lead to higher storage capacity than SDS even at lower concentrations [119].

#### 3.1.2. Influence of Nanoparticles

Nanoparticles, thanks to their unique surface properties and ability to influence transport phenomena, can act as KHPs, improving the rate of hydrate formation, gas storage capacity, and reducing induction times [120–122]. Among all the different nanoparticles, considerations will be given to alumina NPs, silver NPs, zinc oxide NPs, copper oxide NPs, iron oxide NPs, silica NPs, graphene oxide nanosheets, and graphite nanoplates.

The effect of alumina nanoparticles has been investigated when they are added together with surfactants like alkyl polyglucosides (APG) or SDS, showing only a slight improvement in storage density [123], but a synergistic effect in the reduction in induction time, favoring nucleation, when added as a porous powder [124]. Although the influence is positive, it has been found that, regarding the storage density, the improvement is mainly related to the surfactants and their concentration [120].

Silver NPs have a strong influence on methane hydrate formation [125], but regarding $CO_2$ hydrates, they are not as effective in affecting induction time and storage density [126,127]. Nevertheless, molecular dynamics simulations have demonstrated that nanoparticles decrease $CO_2$ agglomeration, increase diffusion and migration to interfaces, and enhance the hydrate growth rate, thanks to their high thermal conductivity, but only at an appropriate concentration of AgNPs; otherwise, they could cause the opposite effect, due to physical blockage of carbon dioxide migration [128].

Other interesting compounds are graphene oxide nanosheets (GO), which are used together with tetra-n-butyl ammonium bromide (TBAB). They act by bonding TBAB ions through the carboxyl groups, delaying TBAB occupation of cavities, improving gas storage,

heterogeneous nucleation and water conversion [129]. A similar result is obtained using graphite powder in addition to SDS [120,129,130].

Although zinc oxide nanoparticles are intensively studied, they find a substantial application only with methane hydrates, where they are applied together with surfactants like SDS [131]. They still have a positive influence on the formation of $CO_2$ hydrates, but their performance is lower than that of other nanoparticles [120]. Relevant studies of zinc oxide nanoparticles are focused on their combined effect with different kinetic promoters such as CTAB and TBAF [132] and thermodynamic promoters like THF, which has a strong influence on $CO_2$ hydrates stability [133].

Copper oxide nanoparticles present behavior like that of alumina ones, showing a relevant positive influence only in the reduction in induction time [120]. A peculiar behavior is exhibited by $Fe_3O_4$ nanoparticles, which increase the conversion of water into hydrate yield; this phenomenon is further enhanced by the application of a magnetic field, thanks to magnetic properties of iron [120,134].

Another example of nanoparticles on which different studies have been conducted is silica ones. In fact, they can be functionalized with a variety of compounds, similarly to other nanoparticles, like $SiO_2$-NPs, and good results in terms of induction time and gas consumption are obtained with an amino group containing functionalization [121].

To improve hydrate-based $CO_2$ capture, additives composed of $SiO_2/Al_2O_3$ nanoparticles (NPs) and tetrabutylammonium bromide (TBAB) were proposed by Z. Cheng et al. [135] demonstrating an improvement in kinetic performance due to the presence of NPs. In this case, the uniform dispersion of NPs during the nucleation step provides a large number of sites for heterogeneous hydrate nucleation (Figure 12), enhancing the ability to break hydrogen bonds between water molecules, thus accelerating hydrate nucleation. In addition, the study of the peaks corresponding to the O–H vibration detected between 3000 and 4000 $cm^{-1}$ by Raman spectroscopy, demonstrated that the presence of NPs increases the destruction of hydrogen bonds between water molecules.

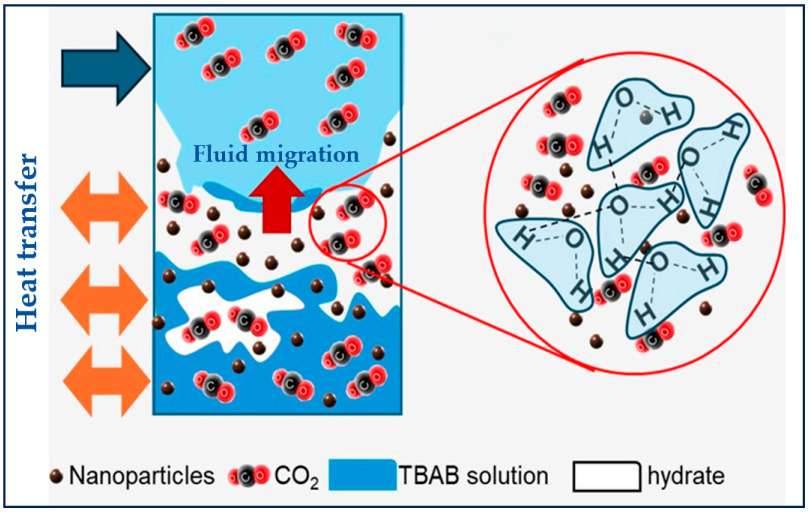


**Figure 12.** Schematic diagram of hydrate formation in the presence of NPs adapted from [135].

However, the specific effect of each nanoparticle depends on its concentration, morphology, surface properties, and the possible presence of other additives such as surfactants, highlighting the complexity of the interactions in these multiphase systems.

### 3.1.3. Memory Effect on Gas Hydrates

Among all the different factors affecting carbon dioxide hydrates or gas hydrates in general, there is one that still lacks a precise explanation: the memory effect. It is a

phenomenon whereby gas hydrates tend to reform more readily in solutions where they have previously formed. The induction times are reduced and the temperatures at which they form are higher [136]. Several attempts to develop theories have been made and they can be resumed in four main theories.

The first proposed mechanism for the memory effect was related to the residual structure hypothesis according to which different retained structures after decomposition, can provide better nucleation sites for the formation of gas hydrates during subsequent synthesis [137]. In fact, the altered residual structure can act as a kinetic promoter and influence the nucleation and growth kinetics of $CO_2$ hydrate in the subsequent hydrate formation cycle.

The first one states that it is due to remaining gas hydrate structures residual in solution, acting as seeds for the subsequent nucleation [137–141], however, it is the least likely to be true among the theories, both due to thermodynamic factors and the observation that using different reactors, under the same conditions, affects the degree of the memory effect [136,142]. The guest gas supersaturation theory hypothesizes that the diffusion of the gas is slowed, and it is considered the most probable to occur, since it does not contradict thermodynamic laws [136,143]. According to the impurity imprinting hypothesis, impurities on the surfaces of the container become conditioned during the initial hydrate formation, enhancing their effectiveness as nucleation sites in subsequent formation cycles [136,139,144,145].

The most recent theory (the nanobubble hypothesis) proposes that nanobubbles generated during hydrate decomposition serve as nucleation sites. These interfacial nanobubbles, particularly those adhering to solid surfaces, enhance the gas–liquid interfacial area, promoting heterogeneous nucleation [145,146]. The $CO_2$–water interfaces of the nanobubbles can act as nucleation sites and thus can influence the distribution, accumulation, and growth of $CO_2$ hydrates. Furthermore, the induction time can be influenced by the water memory effect with a time delay for the onset of hydrate nucleation that can be altered due to past interactions of water with the surrounding environment [147] (Figure 13a). Another hypothesis for the water memory effect is the reduction in water salinity with each cycle of hydrate formation and dissociation, which, by influencing both $CO_2$ dissolution and the phase diagram, enhances hydrate formation in the subsequent cycles as illustrated in Figure 13b [146]. To date, no single hypothesis has been able to comprehensively account for the memory effect completely. This suggests that multiple contributing mechanisms may be acting together, or that the true origin of the phenomenon lies beyond the scope of current theoretical models [136].

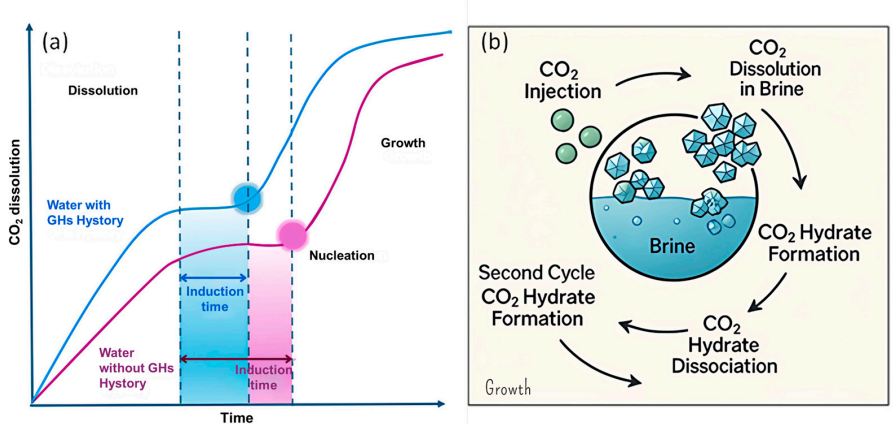


**Figure 13.** (**a**) Representation of the memory effect in the $CO_2$ hydrate formation process during dissolution, induction, and growth. (**b**) Impact of the memory effect on brine salinity and $CO_2$ hydrate formation/dissociation at the pore scale adapted from [146].

3.1.4. Synergistic Effects with Other Gases

Another factor influencing the formation of $CO_2$ hydrate is the presence of other gases either in the air or in the hydrate structure. The substitution of methane with $CO_2$ in the hydrate's structure was proposed as an efficient way to recover $CH_4$ from reservoirs that are naturally present in cold regions [148], this is made possible thanks to the fact that $CO_2$ hydrate are stable at lower pressure than methane hydrates (i.e., the heat of $CO_2$ hydrate formation is higher than the heat of dissociation of $CH_4$) [149]. Given that $CO_2$ occupies the cavities where $CH_4$ was previously present, in this case, there is also the advantage of maintaining the stability of the structure, avoiding slope failures [150]. Another factor to consider is the exothermic nature of $CO_2$ hydrate formation which should be controlled in order to avoid raising the temperature above 10.5 °C to prevent $CO_2$ dissociation. Theoretical limit for $CO_2$ is 64% [151], but an experimental study by Lee et al. [152] showed that no more than 50% of methane can be recovered [153,154]; however, it is still possible to change this value by the addition of other additives [155]. One important aspect to consider when replacing $CH_4$ with $CO_2$ is that methane has a global warming potential 20–30 times greater than that of carbon dioxide. Therefore, the environmental implications of such substitution must be carefully assessed [156]. $CO_2/CH_4$ swapping in gas hydrates occurs through fundamentally different mechanisms depending on whether the system is in the liquid water regime (near or above 0 °C) or in the ice regime (well below 0 °C, with no liquid water present).

In the first case, the mechanism is primarily interface-driven, dominated by processes at the gas–liquid interface. The swapping process is limited by a mass transport barrier created by the formation of a hydrate film, which restricts the diffusion of $CO_2$ through the hydrate surface. This pathway involves the partial dissociation of $CH_4$ hydrate, followed by the formation of a $CO_2$-rich outer shell. A concentration gradient then drives the diffusion of $CH_4$ out of the hydrate structure. The presence of liquid water facilitates this process; however, as water is depleted, the process slows down and the ice regime becomes dominant [157–161].

In the ice regime, where no liquid water is present, swapping occurs via solid-state exchange. In this case, $CO_2$ slowly penetrates the hydrate matrix, and $CH_4$ is released without the need for a gas–liquid interface. Defects in the crystalline structure of the hydrate facilitate the formation of porous $CO_2$ hydrate. This process occurs without dissociation, so the overall structure remains intact. This phenomenon can also occur at temperatures above 0 °C, but with a lower impact compared to interface-driven swapping [152,162–164].

Another example is mixed $CO_2$-$N_2$ hydrates, these are also being studied because both $CO_2$ and $N_2$ are the main constituents of flue gas and so many studies have proposed the formation of hydrates for their capture as a suitable option [151,165]. Lee et al. [70] through DSC, pXRD, and Raman spectroscopy tested the stability of a mixture of mixed $CO_2$-$N_2$ hydrates, with a 90% to 10% ratio, respectively, for $N_2$ and $CO_2$.

Yao et al. [166] studied the mixed hydrate $CO_2/N_2$ under marine $CO_2$ sequestration conditions to evaluate phase equilibrium and cage occupancy through the analysis of the thermodynamic characteristics of the mixed hydrate. Among the environmental effects, the study analyzes the influence of gas–liquid ratios, pressure–temperature gradients and the degree of hydrate formation on the phase equilibrium, kinetics, and thermodynamic stability of hydrates. In this case, excess water enhanced $CO_2$ dissolution, increasing the thermodynamic barrier for hydrate formation and reducing their total composition. Furthermore, hydrate heterogeneity affects the efficiency of $CO_2$ capture and the stability of sequestration under variable environmental conditions. $CO_2/N_2$ injection into marine sediments to form gas hydrates significantly reduces costs and improves environmental

persistence. In Figure 14a a schematic representation is reported for $CO_2$ rich-hydrates and $N_2$ rich-hydrates referred to thermodynamic stability.

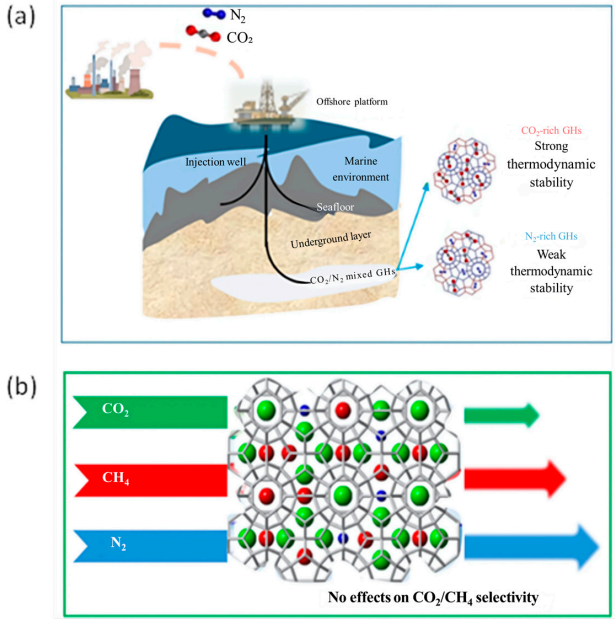


**Figure 14.** Schematic representation for (**a**) $CO_2$-rich hydrates and $N_2$-rich hydrates in marine sediments referred to thermodynamic stability adapted from [166]; (**b**) the impact of $N_2$ concentration on ternary gas hydrate formation for $CH_4$ production and $CO_2$ sequestration adapted from [167].

Recently Mok et al. [167] investigated the formation behavior of $CH_4$ + $CO_2$ + $N_2$ gas hydrates, analyzing the impact of $N_2$ concentration kinetically and thermodynamically by measuring the three-phase equilibrium of the hydrates and analyzing the selectivity of guest molecules within the hydrate structure (Figure 14b). The results demonstrated that the inclusion of $N_2$ reduces the gas consumption and the conversion to hydrate due to a thermodynamic inhibitory effect. Furthermore, the amount of $N_2$ trapped in hydrates increased with its initial concentration in the vapor phase but did not significantly affect the encapsulation behavior of $CO_2$ and $CH_4$. Indeed, the ratio of $CO_2$ to $CH_4$ remained stable both in the vapor phase and in hydrates, regardless of the $N_2$ concentration. These results provide useful insights for $CO_2$ sequestration via hydrates and natural gas production, suggesting that $N_2$ addition could have strategic benefits for $CH_4$ recovery efficiency and gas transport.

### *3.2. Inhibitors of $CO_2$ Hydrate Formation*

Depending on their main effects, the inhibitors can be divided in three different groups: thermodynamic inhibitors (THIs), kinetic inhibitors (KHIs), and antiagglomerants (AA).

Thermodynamic inhibitors were the first class to be applied to avoid the obstruction of pipelines caused by the formation of $CH_4$ hydrates [141]; THIs consist of either highly polar molecules (like methanol or ethylene glycol) [168,169] or ions (salts, which will be discussed more in depth in Section 4.1.3) [170]. These compounds can bind with water either via hydrogen bonding (for polar molecules) or electrostatic interaction (for salts), thus reducing the water able to form a hydrate with the gas molecules and so causing a shift in the phase boundary away from the formation operating condition [171]. The inhibition effect is highly dependent on the ability of the THI to bind with water [169]; for ionic species there is a stronger inhibitor effect for multivalent ions than monovalent ones, a similar effect is seen for polar molecules (it can be taken as an example the fact that ethylene glycol, a molecule with two -OH groups is a better inhibitor than ethanol) [172].

That said some thermodynamic inhibitors, when present at low concentrations can act as promoters [173]. Considering the mechanism in which THIs act to give an efficient inhibition they need to be added in high concentrations [174].

The two other types of inhibitors are also defined as low dosage hydrate inhibitors; in contrast to THIs they can be used in concentrations less than 1% (mass/mass) [175]. Kinetic inhibitors are mainly polymers or copolymers that are water soluble, the most common ones are polyvinylpyrrolidone (PVP) and polyvinylcaprolactam (PVCap) [176]. KHIs, in this case, act as hydrate antinucleators, by binding to the surface of the hydrate nuclei [177]. The binding mechanism remains unclear to this day unclear, as some studies report that the inhibition efficiency is dependent on the presence of amino groups on the KHI [178]; in other studies, it was suggested that the inhibition is molecule dependent [179]. An interesting category of KHI are antifreeze proteins (AFPs), produced by some microorganisms. These proteins are of particular interest because they can be used as a green approach in the inhibition of the $CO_2$ hydrate formation, while maintaining an efficiency comparable to the other KHIs [112,180]; the effect of AFPs will be discussed more in detail in Section 4.4.

Antiagglomerants are surface active materials that prevent hydrates from further agglomeration [168]. The operating mechanisms change depending on the AA structure: for quaternary antiagglomerants (with hydrophilic head groups and hydrophobic tail groups), the hydrophilic part binds to the hydrate surface and the hydrophobic tail keeps the hydrates nuclei away from each other and increases the dispersion of the particles in the hydrocarbon phase [181]. The other class of AAs is able to form an emulsion with water (water in oil emulsion) [182] and, considering the hydrate formation is carried on the liquid phase, a reduction in the formation rate can be observed.

## 4. Effects of Naturally Occurring Compounds on $CO_2$ Hydrate Formation

Seawater is considered as one of the most interesting media for the formation and subsequent stocking of hydrates in general, primarily because of the relatively low temperature and high pressure of the seabed. It is important, however, to consider the composition of the seawater environment, as many of the compounds present in seawater can act either as promoters or inhibitors [183].

In the following paragraphs, in addition to the various additives mentioned above, the effect that some constituents of seawater (both organic and inorganic), as well as the characteristics of sediments, on the formation of $CO_2$ hydrates are described. In addition, some of the most common methods for their determination are reported.

### *4.1. Inorganic Fraction*

#### 4.1.1. Natural Hydrate-Bearing Sediments

To introduce the role of sediments in the stability and formation of gas hydrates, it is essential to first understand the characteristics of natural hydrate-bearing sediments. As previously discussed, gas hydrates occur naturally in cold environments such as deep-sea regions and permafrost zones, where they contribute significantly to sediment stability. It is estimated that the vast majority of natural hydrates are located in deep marine sediments, while less than 1% are found in permafrost zones [184]. However, some studies suggest that this percentage may be slightly higher, approaching 1%. In addition, gas hydrates beneath the Antarctic ice sheet may further increase global estimates of gas stored in hydrate form by approximately 4–24% [185].

Hydrate reservoirs are typically categorized into two types of sediments: fine-grained sediments (median particle size < 62.5 μm) and coarse-grained sediments (median particle size > 62.5 μm). Most research has focused on the latter, as coarse-grained sediments exhibit higher permeability, facilitating methane extraction and making recovery more

economically viable [186]. However, over 90% of natural gas hydrates globally are found in fine-grained sediments, which have significantly lower permeability, posing substantial challenges to recovery operations [186,187]. Particle size also affects hydrate saturation: coarse sediments can reach saturation levels up to approximately 70%, depending on the encapsulated gas type, while fine-grained sediments typically exhibit lower saturation values, ranging from 10 to 25% [184].

The morphology of gas hydrates varies significantly depending on the type of sediment. In coarse-grained sediments, hydrates typically occur as pore-filling structures, dispersed throughout the sediment matrix. In contrast, hydrates in fine-grained sediments tend to manifest as veins, nodules, chunks, or cementing layers between particles. In shallow seabed environments, hydrate morphology is further influenced by the migration of accumulating fluids. In permafrost regions, hydrate structures are generally classified as either pore-filling, dispersed within small pores and not visible to the naked eye, or fracture-filling, which form clusters that can be observed macroscopically [188]. To investigate hydrates in smaller pores, seismic velocity measurements and electrical resistivity logging are commonly used, as hydrate distribution notably affects these parameters [186]. The presence and saturation of hydrates contribute to increased skeletal stiffness of the host sediments, resulting in elevated elastic wave velocities [189]. Additionally, the bulk specific heat of a sediment formation depends on the mass fractions and specific heat capacities of the mineral matrix, pore water, and gas hydrate. These properties significantly affect transient heat flow behavior, raising important safety considerations—particularly during drilling operations.

An interesting characteristic of gas hydrates is their intrinsic thermal conductivity, which is nearly four times lower than that of ice. Additionally, clay-rich sediments exhibit thermal conductivities in the range of 0.72–0.83 W/(m·K), significantly higher than those of sandy sediments, a property that may facilitate the dissipation of heat generated during hydrate formation [190]. However, it is also essential to consider that hydrate dissociation can substantially alter the physical properties of the host sediment, particularly its geothermal and mechanical behavior, potentially leading to severe geohazards such as sediment deformation.

Changes in ocean and atmospheric temperatures can destabilize gas hydrate formations, triggering dissociation processes and methane release. This not only exacerbates greenhouse gas concentrations but also significantly alters the geomechanical properties of the host sediments. As a consequence, several geohazards may arise, including wellbore instability, submarine landslides, seabed collapse, and compromised reservoir integrity [191]. In permafrost regions, where ice and hydrates coexist, dissociation induced by global warming can occur simultaneously at both the top and base of the hydrate stability zone, zones which tend to be relatively narrow. Conversely, in marine environments, dissociation is generally restricted to the base of the hydrate layer [191]. In addition, $CH_4$ exerts a significant influence on global warming, with a radiative forcing potential approximately 20–30 times higher than that of $CO_2$. Consequently, it is essential to monitor variations in bottom water temperature and to identify the environmental parameters that may induce $CH_4$ release from gas hydrates. To date, however, there is no conclusive evidence indicating that methane released from hydrates has reached the atmosphere [156].

#### 4.1.2. Influence of Sediments

Most naturally occurring gas hydrates are found as solid deposits within porous sediments on the ocean floor. These porous environments exhibit a high specific surface area and are notably influenced by interfacial phenomena, such as strong surface tension and capillary-driven coalescence. Over time, research into the behavior of gas hydrates

has developed to include studies using synthetic porous materials like porous silica and glass [56,192–196]. Although the effect of porous media is generally considered to facilitate milder formation conditions, some studies claim the opposite, claiming that using reproduced porous sand samples, gas hydrates need higher pressure and lower temperature [197]. This contradiction is related to the fact that the variation in the dimensions of sediment and its pores strongly influence the results, showing the need to find the optimum granulation for each type of sand. Generally, it has been found that finer particles favor the kinetics of water conversion into hydrates [198–201] and $CO_2$ conversion to hydrate [202].

In addition to pore size and number, the composition of the sediment also affects the phase equilibria of gas hydrates thanks to the secondary interaction between water and sand. Most research studies have demonstrated that the addition of natural sediments positively influences the formation of gas hydrates, proving that the usage of heterogeneous and difficult-to-reproduce samples is fundamental to avoid bias [203,204]. In particular, it has been found that talc and montmorillonite inhibit the formation of hydrates due to the release of cations ($Na^+$, $K^+$, $Ca^{2+}$) [201]. Silica, which is generally the most abundant component of natural sediments, regardless of the particle size, instead shows a positive influence [201,203].

Giovannetti et al. [56] used Raman spectroscopy to monitor the effects of salt, sediment and temperature on the OH vibrations of liquid and frozen water. Experiments demonstrated that porous sand promoted the formation of hydrates, counteracting the inhibitory effect of salt and facilitating heat transfer. Furthermore, the presence of sand altered the equilibrium conditions of hydrates, facilitating their formation at milder temperatures than those reported in the literature. Comparison of experimental data confirmed the role of sand as a promoter of the process.

Gurjar et al. [205] investigated the impact of clay content, salinity, and water saturation in clay−sand sediments on the kinetics of $CO_2$ hydrate formation and sequestration capacity. By considering the potential chemical difference in water to be the driving force and the effective surface area of porous materials as the interface area for hydrate formation, the scholars proposed a new kinetics model. The calculated results accurately predicted the formation rates of $CO_2$ hydrates under various conditions.

Clay minerals (e.g., montmorillonite, kaolinite, illite) exhibit dual roles in gas hydrate systems, acting as thermodynamic inhibitors while simultaneously promoting hydrate nucleation kinetics. Key factors affecting their behavior include the nature of functional surface groups, the composition of interlayer cations, and the extent of organically coated material.

The inhibitory effect of clay minerals on gas hydrate formation is primarily attributed to the reduction in water activity resulting from capillary forces within clay pores and interactions between interlayer cations and water molecules. Conversely, the promotion effect is associated with the presence of Si–O rings, which facilitate gas hydrate nucleation. This kinetic enhancement is further amplified through synergistic interactions between clay minerals and associated organic matter, leading to a reduction in the induction time for hydrate formation. Recent research has explored hybrid materials combining clay minerals with engineered nanostructures, offering promising potential for improving hydrate formation efficiency under complex environmental conditions, such as those found in seawater systems [190].

Pore-scale models are used to simulate the movement, reactivity, and formation of $CO_2$ hydrates within the intricate architecture of porous media. These models consider key factors such as pore geometry, capillary effects, and multiphase flow, offering valuable insights into gas migration, hydrate nucleation, and the influence of sediment properties on storage efficiency. Advanced simulations often incorporate thermal, hydraulic, and mechanical interactions, and can be further enhanced through machine learning techniques

to predict hydrate behavior under variable environmental conditions. Nevertheless, natural porous media exhibit highly complex and heterogeneous pore structures, and many existing models, despite their sophistication—struggle to fully capture the intricacies of hydrate behavior in such systems [206].

Research in this area encompasses experimental investigations into hydrate nucleation, growth, and dissociation at the pore scale. Moreover, several studies have examined how different variables affect hydrate kinetics, storage potential, and the long-term stability of the reservoirs.

#### 4.1.3. Influence of Salts

Water (either pure or seawater) is essential in hydrate formation, and its chemical composition and salinity significantly impact the conditions at which hydrates are stable. Seawater contains various dissolved salts, with the most common ions being $Na^+$, $Cl^-$, $Mg^{2+}$, $Ca^{2+}$, and $SO_4{}^{2-}$. Numerous studies have examined how these electrolytes influence the formation and dissociation of hydrates [207,208]. Dissolved salts act as thermodynamic inhibitors, shifting the hydrate equilibrium by raising the pressure or lowering the temperature required for hydrate stability. Furthermore, it is well established that these salts do not incorporate into the hydrate lattice, which opens the possibility of using hydrate formation and decomposition processes as a basis for desalination technologies [209,210].

Various computational and experimental research studies have confirmed that salts, especially sodium chloride (NaCl), serve as thermodynamic inhibitors by decreasing water activity and forcing hydrate equilibrium conditions towards lower temperature and higher-pressure conditions, making hydrate formation less likely under normal conditions. For example, using a combination of experiments involving a mixture of quantum mechanical (QM) calculations and molecular dynamics (MD) simulations, it was indicated that $Na^+$ and $Cl^-$ ion hydration shells interfere with water, inhibiting gas hydrate nucleation [211]. In addition to that, sodium chloride has a dual influence on hydrate formation kinetics. Low NaCl concentration is seen to increase the driving force for gas dissolution and hence accelerate hydrate formation to a small extent, while high strengths significantly inhibit hydrate formation by reducing the number of free water molecules [212].

From a mechanical point of view, the presence of salts plays a role in altering hydrate-bearing sediments' integrity as well. It was illustrated that an increase in salinity decreases sediments bearing hydrates' mechanical strength and hence their geomechanical stability in nature, especially in marine environments [213]. In a more extended thermodynamic context, investigations utilized Debye–Hückel theory and virial coefficient corrections to calculate the solubility of gases in salty systems and its influence on hydrate formation [214]. These results reaffirm that salt concentration changes both water structure and gas solubility and decreases hydrate formation rates.

### *4.2. Organic Compounds and Their Impact on Hydrate Stability*

The second class of natural compounds discussed in this review consists of organic molecules; the organic composition of seawater is very complex and remains only partially characterized [215], due to the low concentration of the single species. The most common analytical techniques applied for determination of organic matter are HPLC and GC coupled with MS-spectrometry, voltammetry, fluorescence, and UV-analysis [216]. These techniques, especially HPLC-MS and GC-MS, can identify up to very low concentration of analytes, but in some cases pretreatment of the sample is necessary. Dittmar et al. [217] developed a method for the extraction of DOM (dissolved organic matter) from seawater by carrying out solid phase extraction using sorbents with different hydrocarbon chains

and acquired the extraction of more than 60% and 40% organic matter for coastal seawater and deep seawater, respectively.

Liu et al. [218] characterized the organic compounds of pore water via Fourier-Transform Ion Cyclotron Resonance Mass Spectrometry (FT-ICR-MS) and determined that the most abundant organics were lignin, proteins, amino-sugars, lipids, unsaturated hydrocarbons, and carbohydrates; the same sample of water was then tested for $CO_2$ hydrates formation attributed the promoting effect to the elevated number of S-containing compounds in the organic matter. Other studies report lignin, amides, amine-based compounds and humus to behave as KHP, while lipids and unsaturated hydrocarbons showed an inhibitory effect [219,220]. Park et al. [221] suggested the mechanism of interaction between organic anions and sediments to be of electrostatic nature; when $CO_2$ is added to the water the pH would change, making the effect of organics difficult to predict. Considering that, as was stated in the previous section, the formation of hydrates happens mostly on the interface of sediments, this may result in a serious issue when determining the formation and stability of hydrates in water.

### *4.3. Influence of Amino Acids: Hydrophobic vs. Hydrophilic Effects*

Amino acids (AAs) have gained discrete interest in the last decade for their application in the production of hydrates, either as promoters or inhibitors. The increasing number of studies regarding the application of AAs can be related to their non-toxic nature and biodegradability in the environment, as they do not cause pollution; amino acids, in fact, do not form foam, unlike surfactants [222]. They are the building blocks of proteins, composed of carboxyl group (-COOH), an amino group ($-NH_2$) and a side chain forming. The differences in the structure of the side chain determine the function of the AA. Amino acids can be classified either as non-polar or polar depending on the nature of the side chain [223]; Table 3 reports a list of the amino acids treated in this review, with their proprieties.

**Table 3.** List of natural amino acids discussed in this review, with their relative isoelectric points (IPs), hydropathy index (HI) reported according to the Kyte–Doolittle scale, and classification according to the side chain [224].

| AA | Formula | IP | HI | Polarity |
|---|---|---|---|---|
| Lysine | $H_2N$-$[CH_2]_4$-$CH(NH_2)$-COOH | 9.74 | −3.9 | basic polar |
| Methionine | $CH_3S$-$[CH_2]_2$-$CH(NH_2)$-COOH | 5.74 | 1.9 | nonpolar |
| Valine | $(CH_3)_2CH$-$CH(NH_2)$-COOH | 5.96 | 4.2 | nonpolar |
| Tryptophan | 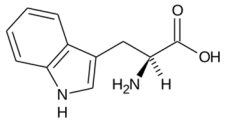 | 5.89 | −0.9 | aromatic |
| Isoleucine | $C_2H_5$-$(CH_3)HC$-$CH(NH_2)$-COOH | 6.02 | 4.5 | nonpolar |
| Histidine | 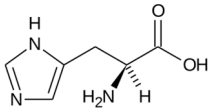 | 7.59 | −3.2 | basic polar |
| Phenylalanine | 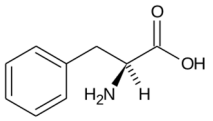 | 5.48 | 2.8 | aromatic |
| Threonine | $CH_3CH(OH)$-$CH(NH_2)$-COOH | 5.6 | −0.7 | polar (no charge) |
| Leucine | $CH_2CH(CH_3)$-$CH(NH_2)$-COOH | 5.98 | 3.8 | nonpolar |
| Arginine | $H_2N$-$C(=NH)$-$NH$-$[CH_2]_3$-$CH(NH_2)$-COOH | 10.76 | −4.5 | basic polar |
| Cysteine | $HS$-$CH_2$-$CH(NH_2)$-COOH | 5.07 | 2.5 | polar (no charge) |

**Table 3.** *Cont.*

| AA | Formula | IP | HI | Polarity |
|---|---|---|---|---|
| Tyrosine | 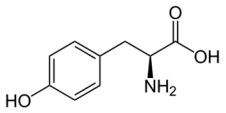 | 5.66 | −1.3 | aromatic |
| Serine | HO-$CH_2$-CH($NH_2$)-COOH | 5.68 | −0.8 | polar (no charge) |
| Alanine | $CH_3$-CH($NH_2$)-COOH | 6 | 1.8 | nonpolar |
| Asparagine | $H_2N$-CO-$CH_2$-CH($NH_2$)-COOH | 5.41 | −3.5 | polar (no charge) |
| Aspartic acid | HOOC-$CH_2$-CH($NH_2$)-COOH | 2.77 | −3.5 | acidic polar |
| Glutamic acid | HOOC-[$CH_2$]$_2$-CH($NH_2$)-COOH | 3.22 | −3.5 | acidic polar |
| Glycine | H-CH($NH_2$)-COOH | 5.97 | −0.4 | nonpolar |
| Proline | 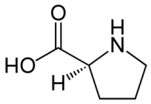 | 6.3 | −1.6 | nonpolar |

Like many other additives, AAs were first introduced as inhibitors for the methane hydrate formation in pipelines. However, only recently have they been found to also have a promoting effect depending on two main factors: concentration of the AA and nature of the side chain [225]. The first study on the application of AAs as promoters was conducted recently by Liu et al. [226], where they used various amino acids at low concentration to promote the formation of $CH_4$ hydrates.

The mechanism of interaction between amino acids and water for the hydrate formation remains unclear to this day; it was theorized that the acting mechanism is similar to the one of $CH_4$ hydrates, as with the addition of surfactants (in fact AAs are also amphiphilic in nature): the polar groups make the molecule soluble in water, while the hydrophobic chain adsorbs at the hydrate interface reducing the surface tension facilitating the nucleation; if the side chains are long enough, there is an additional promoting effect that can be associated with an increase in the contact surface between water and the gas molecules [227,228]. The promoting effect is however limited, above a certain concentration, which varies depending on the AA; the hydrate accumulates on the surface boundary and forms a layer that hinders the hydrate formation by lowering the mass transfer [225].

The behavior of AAs in hydrate formation varies depending on the gas guest molecule. For example, Kumar et al. [229] used L-histidine as a kinetic promoter for the formation of $CH_4$ hydrates; on the contrary, Roosta et al. [230] found the same AA to act as an inhibitor in the production of $CO_2$ hydrates.

Sa et al. [231] studied the inhibiting properties of some hydrophobic amino acids (L-glycine, L-alanine, L-valine, L-leucine and L-isoleucine) with the concentration going from 0.1 to 1 mol%. It was determined that there is no change in the inhibition effect as the concentration of AA increases; however, they found glycine and L-alanine to be effective in reducing the memory effect. They also determined a correlation between the increasing hydrophobicity of the AA and a higher kinetic inhibiting effect, which is opposite to the trend that can be observed when using AAs as THIs [232].

Sa et al. [233] in a subsequent study evaluated the inhibition effect of five amino acids (asparagine, alanine, aspartic acid, phenylalanine, and histidine) on $CO_2$ hydrate formation at concentrations between 0.01 and 0.1 mol%. They determined asparagine and aspartic acid as the most efficient inhibitors, with histidine followed by alanine and phenylalanine in order of inhibition effect. They also noted that histidine was able to delay $CO_2$ hydrate nucleation time and growth better than alanine. Phenylalanine had no significant impact on the hydrate nucleation process.

The role of leucine in the formation of $CO_2$ hydrates is however unclear. Some studies reported the leucine to possess promoting abilities, probably because of the leucine favoring the growth of the hydrate on the wall of the reaction vessel [227]. However, it was also reported that at a concentration of leucine above 1% wt., the hydrate formation is hindered due to the amino acid precipitation, due to $CO_2$ hydrate formation [234].

Yodpetch et al. [235] investigated the effect of three amino acids, leucine, valine, and methionine, on $CO_2$ hydrate formation. The one with the highest hydrate formation rate was methionine; leucine had a slower rate due to a delayed growth in the first 15 min; for what regards gas uptake no significant increase was observed for the amino acids tested. The promoting effect of methionine and leucine was also confirmed by Srivastava et al. [236]; in the same article, an increase in the uptake of $CO_2$ in the presence of a mixed solution of methionine, leucine, and lecithin was also observed. Additionally, Prasad et al. [237] studied the effect of methionine and phenylalanine at low concentration (0.5 wt%), confirming the promoting effect of methionine. However, phenylalanine showed a significant reduction in gas uptake. Khandelwal et al. [238] tested tryptophan at different concentrations for $CO_2$ capture and storage; with 300 ppm of said amino acid, the conversion rate of water to hydrate was 78%, with the shortest induction time among the tested concentrations. Contrasting results were also found for isoleucine. Sa et al. [231], while testing different amino acids as THIs, determined that both leucine and isoleucine have a weak promotion effect on $CO_2$ hydrates formation. On the contrary, Liu et al. [239], while still using isoleucine, observed a significant increase in the $CO_2$ hydrate formation when adding low concentrations of the amino acid (0.2 wt%).

Prasad et al. [240] tested 5 amino acids (valine, cysteine, threonine, methionine, and phenylalanine) at a concentration of 0.5 wt%; only valine, cysteine, and methionine were determined to have a significant effect on $CO_2$ uptake (around a 20% increase), while phenylalanine and threonine had negligible influence. In a subsequent study [241], the same authors evaluated the effect of L-methionine and L-phenylalanine (0.5 wt%) on $CO_2$ capture, providing further confirmation of the low impact of phenylalanine on hydrate promotion and the strong promoting effect of methionine. In this case, the combination of both methionine and phenylalanine further increased the hydrate formation, reaching up to 90% gas to hydrate conversion rate and above 85% water to hydrate conversion after one hour.

The promotion/inhibition effect of amino acids is highly dependent on the guest molecule present; this offers interesting opportunities for mixed gases separation and $CO_2$ capture applications. Another factor that may contribute to the promotion/inhibition effect of amino acids is their side chain length; however, the correlation between the length of the side chain and the inhibition effect of AAs is not well understood. Authors suggest there is an optimum side chain length of hydrophobic amino acid in hydrate kinetic promotion/inhibition [230]. Amino acids with polar side chains usually show better $CO_2$ hydrate inhibition compared to non-polar ones. According to Sa et al. [233], the hydrate nucleation and growth inhibition is also dependent on the hydropathy index, a numerical value of the hydrophobicity/hydrophilicity of the amino acids side chain, commonly used to identify hydrophobic and hydrophilic regions within a protein's structure [242].

### Determination of Amino Acids in Seawater

Amino acids are commonly found in seawater at very low concentrations [243] in combination with the high amount of different substances present, which means that, to detect AAs, water samples require thorough sample treatment prior to analysis.

Early methodologies reported in the literature predominantly rely on chromatographic techniques, including ion exchange for sample concentration [244] and thin-layer chro-

matography (TLC), which enables sensitive detection (Riley et al. [245] reported a detection limit of 0.1 μg/L); furthermore, freeze-drying and evaporation have often been employed to pre-concentrate amino acids prior to ion exchange chromatography applied to seawater matrices [246–248]. Another study by Litchfield et al. [249] involved the separation by TLC-made dansyl derivatives of amino acids, from both seawater and freshwater samples, to improve the efficiency of the method.

Currently, the most widely used method for detecting amino acids in seawater is fluorimetric analysis of derivatized AAs; derivatization is necessary, since the only fluorescent amino acids are tryptophan, tyrosine, and phenylalanine. Functionalization is usually carried out with a variety of molecules, most notably o-phthaldehyde (OPA) and ninhydrin. Gentle filtration is always recommended to prevent the release of amino acids after sampling.

The OPA method is the simplest and most widely used, as free amino acids can be determined with easy sample preparation while still retaining good sensitivity. Since its introduction, the method has been substantially improved through much research; the most notable improvements include higher stability of the derivatives, reduction/elimination of many interferences, resolution of certain pairs of amino acids, improved detection limit of the AAs, and determination AAs enantiomers present at trace levels [250].

A recent study also reports on the application of metal complexes as fluorescent and colorimetric chemosensors for the detection of amino acids [251].

### *4.4. Peptides and Protein-Based Modulation of Hydrate Growth*

Regarding proteins, their role is well established as KHIs in the formation of hydrates in general [252]. Proteins are rich in polar functional groups and so can form hydrogen bonds with water molecules, thus causing an inhibition in the hydrate nucleation. In addition, protein derivatives can promote hydrate formation by changing the surface tension of the aqueous solution, allowing more water to be converted into hydrate within a shorter time period [253]. Kelland et al. [254] tested various peptones (intermediates formed during the hydrolysis of proteins) as KHIs for the formation of THF hydrates and related the inhibiting properties to three main factors analogous to commonly used polymers: molecular weight, molecular weight distribution, and the ratio of amino acid residues.

Antifreeze proteins (AFPs) are a group of proteins of particular interest, not only for their application as thermodynamic hydrate inhibitors, but also for their high biodegradability and non-toxic nature [255]. Since commercially prepared AFPs are expensive, the use of organisms capable of producing them in situ presents an appealing prospect [256].

AFPs were isolated for the first time by Scholander from Arctic fish [257]. These proteins are produced by various organisms such as fish, insects, plants, bacteria, and fungi as a mechanism to survive low temperatures in cold environments [258–260]. AFPs exhibit thermal hysteresis activity, which creates a difference between the freezing and melting points of ice crystals; the magnitude of this effect varies depending on the efficiency of the AFPs [261]. By binding to ice crystals, AFP enhances the resistance of the organism to freezing [262]. Because of this property, AFPs have been extracted and their effect on ice crystals was extensively studied in multiple works [263]. MD simulations are commonly used to investigate the mechanisms by which these proteins bind to ice crystals [264,265].

Hudait et al. [265] used antifreeze proteins extracted from insects to investigate the role of hydroxyl and hydrophobic groups in binding to the ice surface. They determined that both hydrogen bonds and hydrophobic interactions are essential for the AFPs to attach to the ice. An interesting type of AFP is Winter flounder AFP (wf-AFP), found in fish; it is a protein with low molecular mass and high flexibility/deformability. According to the study conducted by Zeng et al. [266], wf-AFP has an inhibiting effect on propane and THF

hydrate. Maxy et al. [267] expanded the research by comparing the hydrate formation times with wf-AFP to those with type I AFPs, finding the former to be five times longer than the latter. Furthermore Al-Adel et al. [268] tested wf-AFP on methane hydrate and found it to be a more effective inhibitor than PVP and PVcap. AFPs from different species exhibit different values of thermal hysteresis activity; consequently, their effects on hydrates may also vary [269].

The inhibition properties of AFPs on hydrates formation have not been deeply studied. Zhou et al. [270], for example, showed that the addition of low concentration of type-III AFPs was able to significantly decrease the dissolution rate of gas into the solution, resulting in a reduction in the formation of $CO_2$ hydrate by about 35%. Zhang et al. [271] carried out MD simulations to calculate the inhibition effect of a mixture composed of methanol and wf-AFP; the results indicate that the combined effect of the two inhibitors was able to significantly reduce dissolved $CO_2$ as the gas source, thus prominently inhibiting hydrate growth to near stagnation.

Determination of Proteins and Peptides in Seawater

The older methods for the measurement of protein in natural waters are usually based on the presence of aromatic amino acids in the protein. The total protein count is calculated on the average content of tryptophan, tyrosine, or phenylalanine. A representative method of this type is the Folin reagent method, published by Lowry et al. [272], which uses the Folin reagent (sodium 1,2-naphthoquinone-4-sulfonate); proteins concentration is then determined via UV-Vis spectroscopy [273]. Although this method is highly sensitive, the intensity of color varies with the type of protein, and for this reason, a strict proportional correlation between color intensity and protein concentration is not possible [272]. However, these methods are only useful in freshwater and in some coastal regions, as they are not sensitive enough for the low protein concentrations found in the oceanic waters.

Packard and Dortch adapted a fluorescence method based on fluorescamine, for the determination of free and combined amino acids (depending on the pH of the solution) originally proposed by Udenfriend [274]. The steps are reported as follows: first 100 mL of seawater were filtered through a 2.5 cm Gelman glass filter, then the filter was grounded in 3 mL of water with a Teflon-glass tissue grinder. A total of 1 mL of this homogenate was added to 3 mL of borate buffer, to which fluorescamine was then added dropwise under stirring on a vortex mixer. Fluorescence was then measured spectrofluorometrically at 480 nm with the excitation wavelength set at 390 nm. Peptides and amino acids exhibited maximum fluorescence at pH 7 and 9, respectively.

Another method for the detection of proteins was proposed by Tanoue [275], and the procedure consists of three steps: first, concentration of dissolved proteins from seawater by tangential flow ultrafiltration; second, further concentration and purification by precipitation with trichloroace-tic acid; and lastly, separation and detection of dissolved proteins by sodium dodecyl sulfate-polyacrylamide gel electrophoresis. Using this method, it was possible to extract only a limited amount of proteins (less than 30).

### *4.5. Role of Humic Substances in Hydrate Formation in Marine and Geological Environments*

Humic substances are a complex mixture of supramolecules combined with low molecular weight organic compounds containing carboxyl and phenolic-hydroxyl groups, formed during the decomposition of animal and plant matter [276]. The main constituents of humic substances are fulvic acids, humic acids, lignin, fatty acids, and proteins [277]. The terms humic and fulvic acid derive from their different behavior: humic acids are those compounds extracted by alkaline solutions and then precipitated upon acidification; fulvic acids, in contrast, remain in solution after acidification following alkaline extraction [278].

These terms were originally specific to materials isolated from soil; however, has since been extended to marine sediments. It is important to note that materials isolated from the marine environment differ from soil counterparts, at least in $^{13}C/^{12}C$ isotope ratios and presumably in their structure [273].

Several studies have demonstrated both the promoting and inhibiting effects of humic substances on methane hydrate formation [279–281].

The sole study currently available in the literature concerning the effect of humic substances on $CO_2$ hydrate formation is that of Lamorena et al. [219]. Their investigation evaluated humic substances in combination with other organic compounds, such as commercial humic acid, lignin, and amide-bearing molecules, all of which were found to promote hydrate nucleation and growth. It was suggested that supramolecules can associate with water molecules and soil, causing a modification in the arrangement of water clusters, which in turn enhances the formation of $CO_2$ hydrates. Recently, Liu et al. [282] reported an interesting study on fulvic acid (FA), used to achieve rapid formation of $CO_2$ hydrates from liquid $CO_2$ in the marine waters of South China. In this study, a previously unreported phenomenon, called the self-siphoning effect, was demonstrated, where the aqueous solution is "sucked" into the pores of the hydrates, further accelerating their growth. With FA, nucleation and growth of hydrates were completed within 30 min, achieving one of the highest growth rates recorded so far. Fulvic acid thus proves effective even in saline conditions, overcoming the limitations encountered with other additives such as amino acids. These findings open new perspectives on a more sustainable approach to underwater $CO_2$ storage.

Recently, lignin sulfonate has emerged as a compound of interest owing to its elevated surface activity, similar to SDS, combined with its non-toxic nature and favorable biodegradability profile.

Commonly applied as sodium lignosulfonate, it is a byproduct of pulp production, generated by the reaction between wood and a solution of sulfur dioxide and sulfite [283]. It possesses a high number of functional groups that confer amphiphilic properties to the molecule. Yi et al. [284] utilized ligninsulfonate (SL) to promote hydrate-based $CO_2$ capture from a $CO_2/CH_4$ mixture. SL can act as a potential KHP for gas hydrate, due to its low cost, making it an economically viable alternative to other conventional additives. Huang et al. [285] determined that the addition of 1.0 wt.% of sodium lignosulfonate can significantly reduce the induction time the formation of $CO_2$ hydrates, from 66 min for pure water to 5.25 min. This acceleration was attributed to sodium lignosulfonate's ability to form micelles, which provide an increased number of nucleation sites, thus raising the probability of collisions between $CO_2$ molecules and these sites and accelerating hydrate nucleation [286]. In addition to that, the storage capacity of $CO_2$ is increased to almost 2.0 times that of pure water.

### Determination of Humic Substances in Seawater

For the analysis of lignin and its derivatives, a concentration step is usually employed in order to bring the analytes in sample within the detection range of the method and to reduce interferences during the spectrometric analysis. Othman et al. [287] extracted lignosulfonic acids using using emulsion liquid membrane process. Pocklington et al. [288] used a reaction between sediment samples and 1,3,5-tri-hydroxybenzene in alcoholic hydrochloric acid to produce a colored-lignin, which can be identified under the microscope.

Louchouam et al. [289] performed solid-phase extraction (SPE) preconcentration of acidified seawater using a C18 cartridge, followed by capillary gas chromatography (GC) coupled to selected-ion monitoring mass spectrometry of the products of lignin after oxidation by CuO. This method was adapted from Hedges et al. [290] as follows: the sample was

loaded in a vessel containing 1 g of CuO (powdered), 25–100 mg $Fe(NH_4)_2(SO_4)_2 \cdot 6H_2O$ (used as an $O_2$ scavenger), 7.0 mL of 8% (wt/wt) aqueous NaOH. The NaOH solution was sparged for 30 min and sonicated for 1 min prior to loading the samples. Direct spectrophotometric methods are possible for some lignosulfonic acid derivatives; for example, nitroso derivatives can be determined by differential pulse polarography [291]. As a general rule, fluorometric methods are considerably more sensitive than spectrophotometric methods, although they are more difficult to standardize [292].

For the analysis of humic and fulvic acids, the greatest challenge remains the high structural heterogeneity of these compounds. Methods for extracting and analyzing humic and fulvic acids from marine samples are adapted from soil chemistry protocols [293–295]. Among these, the easiest and most cost-effective is the Rhizon sampler, which consists of a porous tube that can extract pore water with minimal disturbance to sediment structure and flow fields. However, its main limitation is a restricted depth resolution, typically no more than 1 cm [296].

Centrifugation represents another method that minimizes the loss of organic compounds [297]. Alternatively, squeezing [298] and pressure retaining methods [299] can be used; the latter category is of particular interest because it can maintain in situ pressure, thereby reducing sample alteration, and enabling multi-depth analysis [300]. Another technique for extracting organics from shallow pore water involves the use of well-point samplers, which have the great advantage of eliminating metal contamination caused by sampler corrosion [301]. Some studies report the use of macroreticular resins to collect high molecular weight compounds from seawater; these resins can also be applied to collect humic and fulvic acids separated from sediments [302]. Among the possible techniques used to characterize humic and fulvic acid ESR, thermal analysis, NMR, spectrophotometry, and GC–MS analysis are the most common [303]. Some methods specific for fulvic acid consist of measuring UV absorption at 400 and 340 nm after removing humic substances or, if the fulvic acids are removed using activated charcoal, they can be determined by alternating current (AC) polarography [273].

Gel permeation chromatography (GPC) is another widely used method for determining the size distribution of humic acids. Since the elution of these materials is influenced by the present functional groups present, this analysis can provide valuable information for subsequent investigations [304].

If a rougher estimation of the seawater composition is acceptable, fluorescence can be used; this approach removes the need for extensive sample preparation [292]. Fluorimetry is also used to measure short-range variability of humic and fulvic acids. However, interference from other fluorescing compounds present in the sample may occur. It is also important to consider that the fluorescence of humic and fulvic acids decreases rapidly when seawater is exposed to sunlight; therefore, fluorescence should be avoided for the analysis of surface waters. For compounds too large to be determined directly via GC-MS, preliminary treatments usually consist of hydrolysis [305] or oxidation [306].

Many of the methods used for lignins can also be applicable to humic acids. For example, pulse polarography after the formation of nitroso derivatives can be used for both humic acids and lignins [291].

## 5. Challenges and Prospects

The implications of this comprehensive review on $CO_2$ capture and sequestration via gas hydrates, especially considering the influence of natural compounds and marine sediments, are significant for advancing sustainable climate mitigation technologies. By elucidating the fundamental mechanisms of hydrate formation, the role of promoters and inhibitors, and the critical impact of marine environmental factors such as sediments,

salts, and organic matter, this work highlights the complex interplay governing hydrate stability and formation. This understanding is essential for optimizing hydrate-based carbon capture and storage (CCS) systems, which could offer a promising, secure, and long-term method for reducing atmospheric $CO_2$ levels.

Moreover, the detailed investigation into naturally occurring molecules, including amino acids, proteins, and humic substances, and their dual roles as either promoters or inhibitors underscores the importance of integrating ecological complexity into technological development. Insights into the memory effect, and synergistic interactions with other gases further inform the design of efficient hydrate systems suitable for varying environmental conditions, such as marine sediments and porous media.

However, several weaknesses are apparent across the reviewed studies. A common limitation is the scarcity of long-term, large-scale experimental data and field studies, which makes the practical implementation of $CO_2$ hydrate-based CCS uncertain. Many experimental conditions remain confined to laboratory scale and idealized setups, which may not fully capture the heterogeneity, multi-component chemistry, and dynamic environmental conditions encountered in marine sediments.

Despite significant advances in understanding $CO_2$ hydrate formation and its potential application in carbon capture and storage (CCS), several critical gaps remain in the literature that warrant further investigation.

Firstly, the complex interplay between natural marine sediment compositions, diverse organic compounds, and hydrate stability is still not fully understood. While the promoting and inhibiting effects of individual additives such as amino acids, proteins, and humic substances have been documented, their synergistic or antagonistic interactions in situ conditions remain largely unexplored. Future research should focus on comprehensive studies that simulate realistic marine environments to unravel these multifactorial influences and their impact on hydrate formation kinetics and stability.

Secondly, much of the current thermodynamic and kinetic modeling relies on idealized assumptions that often do not fully capture the non-ideal behavior observed in natural and engineered systems. The role of chemical potentials, activities, and heterogeneous microenvironments at mineral interfaces and pore scales introduces complexities that existing models inadequately address. Advancing multi-scale experimental and computational approaches, including molecular dynamics simulations integrated with pore-scale modeling, is essential to accurately predict hydrate behavior in natural sediments.

Furthermore, the "memory effect" phenomenon, where previously formed hydrates enhance subsequent hydrate nucleation, lacks a definitive mechanistic explanation. Various hypotheses such as residual structures, nanobubbles, and impurity imprinting have been proposed, but conclusive evidence remains elusive. Elucidating the mechanistic basis of the memory effect through innovative experimental designs and high-resolution characterization techniques will significantly improve hydrate formation control and efficiency.

Lastly, there is a pressing need for scalable and economically viable hydrate formation methods. Although various promoters, inhibitors, and nanoparticles have shown promise in laboratory settings, translating these findings to field-scale applications remains challenging. Future research should prioritize the development of low-cost, sustainable additives and engineering solutions that enhance hydrate formation rates and storage capacities while ensuring environmental safety.

Thus, addressing these identified gaps through interdisciplinary research combining experimental, analytical, and modeling efforts, will be pivotal to optimizing gas hydrate technologies for effective carbon capture and sequestration in marine environments.

Given the urgency of achieving Net Zero emissions by 2050, the findings emphasize the potential of gas hydrates not only for CCS but also for methane recovery through

$CO_2$-$CH_4$ swapping, contributing to cleaner energy resources. Furthermore, understanding the physicochemical and thermodynamic influences from natural sediments and seawater chemistry supports the development of more reliable, cost-effective, and eco-friendly hydrate technologies.

## 6. Conclusions

This review explores the use of gas hydrates as a promising alternative for $CO_2$ capture and storage, with particular emphasis on the influence of natural compounds and marine sediments on hydrate formation.

As the rising concentration of atmospheric $CO_2$ is one of the main drivers of climate change, carbon capture and storage (CCS) technologies are essential to achieving climate neutrality by 2050.

The review summarizes the characteristics of $CO_2$ hydrates, the main characterization techniques, thermodynamic and kinetic aspects and the growth mechanism, the effects of key promoters and inhibitors, as well as the memory effect, a phenomenon in which hydrates reform more easily after their initial formation. It was considered, also, the synergic effect of different gases and in particular the $CO_2/CH_4$ swapping that can occurs via distinct mechanisms depending on temperature conditions. Understanding these mechanisms is essential for optimizing gas exchange strategies in hydrate-based applications.

Special attention is given to the influence of the marine environment: how the presence of sediments affects hydrate formation due to grain size and mineral composition; salts act as thermodynamic inhibitors; and organic compounds such as dissolved organic matter (DOM), amino acids, proteins, and humic substances that can act as either promoters or inhibitors. Particular focus is also placed on sampling and analytical characterization techniques used for the detection and identification of these types of compounds.

The review highlights the potential of $CO_2$ hydrates as a CCS technology, while emphasizing the need for further research to better understand the role of natural compounds and marine sediments. The integration of experimental and computational approaches is crucial for optimizing this technology.

This review is part of the dissemination and communication plan of the project *Reliable long-term $CO_2$ storage as clathrate hydrates in seawater and marine sediments*, funded by the European Union—Next Generation EU, and led by the University of Perugia, the University of Camerino, and the OGS Institute as research units.

**Author Contributions:** Conceptualization, M.Z. and R.G.; data curation: L.R., A.T., M.Z. and R.G.; writing—original draft preparation, L.R. and A.T.; writing—review and editing, M.Z. and R.G.; supervision, M.Z. and R.G.; project administration, M.Z.; funding acquisition, M.Z. All authors have read and agreed to the published version of the manuscript.

**Funding:** This research was funded by PRIN2022PNRR $CO_2$-RESTO (CUP: J53D23015790001, grant number: P2022PF3M4).

**Data Availability Statement:** No new data were created or analyzed in this study.

**Conflicts of Interest:** The authors declare no conflict of interest.

## References

1. Canadell, J.G.; Le Quéré, C.; Raupach, M.R.; Field, C.B.; Buitenhuis, E.T.; Ciais, P.; Conway, T.J.; Gillett, N.P.; Houghton, R.A.; Marland, G. Contributions to Accelerating Atmospheric $CO_2$ Growth from Economic Activity, Carbon Intensity, and Efficiency of Natural Sinks. *Proc. Natl. Acad. Sci. USA* **2007**, *104*, 18866–18870. [CrossRef]
2. Hoegh-Guldberg, O.; Jacob, D.; Taylor, M.; Guillén Bolaños, T.; Bindi, M.; Brown, S.; Camilloni, I.A.; Diedhiou, A.; Djalante, R.; Ebi, K.; et al. The Human Imperative of Stabilizing Global Climate Change at 1.5 °C. *Science* **2019**, *365*, eaaw6974. [CrossRef]

3. Bahman, N.; Al-Khalifa, M.; Al Baharna, S.; Abdulmohsen, Z.; Khan, E. Review of Carbon Capture and Storage Technologies in Selected Industries: Potentials and Challenges. *Rev. Environ. Sci. Biotechnol.* **2023**, *22*, 451–470. [CrossRef]
4. Li, H.; Lau, H.C.; Wei, X.; Liu, S. $CO_2$ Storage Potential in Major Oil and Gas Reservoirs in the Northern South China Sea. *Int. J. Greenh. Gas Control.* **2021**, *108*, 103328. [CrossRef]
5. Zhang, X.; Bai, Y.; Zhang, Y. Collaborative Optimization for a Multi-Energy System Considering Carbon Capture System and Power to Gas Technology. *Sustain. Energy Technol. Assess.* **2022**, *49*, 101765. [CrossRef]
6. Teng, Y.; Wang, P.; Jiang, L.; Liu, Y.; Song, Y.; Wei, Y. An Experimental Study of Density-Driven Convection of Fluid Pairs with Viscosity Contrast in Porous Media. *Int. J. Heat Mass Transf.* **2020**, *152*, 119514. [CrossRef]
7. Trends in $CO_2$—NOAA Global Monitoring Laboratory. Available online: https://gml.noaa.gov/ccgg/trends/ (accessed on 19 June 2025).
8. Roussanaly, S.; Berghout, N.; Fout, T.; Garcia, M.; Gardarsdottir, S.; Nazir, S.M.; Ramirez, A.; Rubin, E.S. Towards Improved Cost Evaluation of Carbon Capture and Storage from Industry. *Int. J. Greenh. Gas. Control* **2021**, *106*, 103263. [CrossRef]
9. Soo, X.Y.D.; Lee, J.J.C.; Wu, W.Y.; Tao, L.; Wang, C.; Zhu, Q.; Bu, J. Advancements in $CO_2$ Capture by Absorption and Adsorption: A Comprehensive Review. *J. $CO_2$ Util.* **2024**, *81*, 102727. [CrossRef]
10. Schnaar, G.; Digiulio, D.C. Computational Modeling of the Geologic Sequestration of Carbon Dioxide. *Vadose Zone J.* **2009**, *8*, 389–403. [CrossRef]
11. Snæbjörnsdóttir, S.; Sigfússon, B.; Marieni, C.; Goldberg, D.; Gislason, S.R.; Oelkers, E.H. Carbon Dioxide Storage through Mineral Carbonation. *Nat. Rev. Earth Environ.* **2020**, *1*, 90–102. [CrossRef]
12. Sun, X.; Shang, A.; Wu, P.; Liu, T.; Li, Y. A Review of $CO_2$ Marine Geological Sequestration. *Processes* **2023**, *11*, 2206. [CrossRef]
13. Gayathri, R.; Mahboob, S.; Govindarajan, M.; Al-Ghanim, K.A.; Ahmed, Z.; Al-Mulhm, N.; Vodovnik, M.; Vijayalakshmi, S. A Review on Biological Carbon Sequestration: A Sustainable Solution for a Cleaner Air Environment, Less Pollution and Lower Health Risks. *J. King Saud Univ. Sci.* **2021**, *33*, 101282. [CrossRef]
14. Rossi, A.; Ciulla, M.; Canale, V.; Zannotti, M.; Minicucci, M.; Di Profio, P.; Giovannetti, R. Constant Pressure $CO_2$ Replacement of $CH_4$ in Different Hydrate Environments: Structure and Morphology. *Energy Fuels* **2023**, *37*, 18968–18976. [CrossRef]
15. Hashimoto, H.; Yamaguchi, T.; Ozeki, H.; Muromachi, S. Structure-Driven $CO_2$ Selectivity and Gas Capacity of Ionic Clathrate Hydrates. *Sci. Rep.* **2017**, *7*, 17216. [CrossRef] [PubMed]
16. Wang, P.; Li, Y.; Sun, N.; Han, S.; Wang, X.; Su, Q.; Li, Y.; He, J.; Yu, X.; Du, S.; et al. Hydrate Technologies for $CO_2$ Capture and Sequestration: Status and Perspectives. *Chem. Rev.* **2024**, *124*, 10363–10385. [CrossRef] [PubMed]
17. Rukh, M.; Rahman, M.S.; Sakib, K.M.N.; Pantha, S.C.; Hasan, S.; Jabeen, M.; Islam, M.S. A Comprehensive Review of Semi-Clathrate Hydrates for $CO_2$ Capture: Characterizations, Mechanism and Role of Promoters. *Carbon. Capture Sci. Technol.* **2024**, *12*, 100217. [CrossRef]
18. Faraday, M. XIV. On Fluid Chlorine. *Philos. Trans. R. Soc. Lond.* **1823**, *113*, 160–165. [CrossRef]
19. Hammerschmidt, E.G. Formation of Gas Hydrates in Natural Gas Transmission Lines. *Ind. Eng. Chem.* **1934**, *26*, 851–855. [CrossRef]
20. Wróblewski, Z.F. Sur La Combinaison de l'acide Carbonique et de l'eau. In *Comptes Rendus de l'Académie des Sciences*; Académie des Sciences: Paris, France, 1882; Volume 94.
21. Yamamoto, K.; Terao, Y.; Fujii, T.; Ikawa, T.; Seki, M.; Matsuzawa, M.; Kanno, T. Operational Overview of the First Offshore Production Test of Methane Hydrates in the Eastern Nankai Trough. *Proc. Annu. Offshore Technol. Conf.* **2014**, *3*, 1802–1812. [CrossRef]
22. Aminnaji, M.; Qureshi, M.F.; Dashti, H.; Hase, A.; Mosalanejad, A.; Jahanbakhsh, A.; Babaei, M.; Amiri, A.; Maroto-Valer, M. $CO_2$ Gas Hydrate for Carbon Capture and Storage Applications—Part 1. *Energy* **2024**, *300*, 131579. [CrossRef]
23. Pei, J.; Chen, J.; Wang, J.; Li, Z.; Li, N.; Kan, J. $CO_2$ Capture Technology Based on Gas Hydrate Method: A Review. *Front. Chem.* **2024**, *12*, 1448881. [CrossRef] [PubMed]
24. Hassanpouryouzband, A.; Joonaki, E.; Vasheghani Farahani, M.; Takeya, S.; Ruppel, C.; Yang, J.; English, N.J.; Schicks, J.M.; Edlmann, K.; Mehrabian, H.; et al. Gas Hydrates in Sustainable Chemistry. *Chem. Soc. Rev.* **2020**, *49*, 5225–5309. [CrossRef]
25. Annavajjala, S.B.; Van Dam, N.; Mahajan, D.; Kosny, J. A Review of $CO_2$ Clathrate Hydrate Technology: From Lab-Scale Preparation to Cold Thermal Energy Storage Solutions. *Energies* **2025**, *18*, 2659. [CrossRef]
26. Liu, T.; Wu, P.; Chen, Z.; Li, Y. Review on Carbon Dioxide Replacement of Natural Gas Hydrate: Research Progress and Perspectives. *Energy Fuels* **2022**, *36*, 7321–7336. [CrossRef]
27. Mahmood, M.N.; Gupta, A.S.; Islam, M.T. $CO_2$ Storage in Natural Gas Hydrate Reservoirs: A Review on Prospects and Challenges Ahead. *Next Res.* **2024**, *1*, 100017. [CrossRef]
28. Asadi, J.; Kazempoor, P. Techno-Economic Analysis of Membrane-Based Processes for Flexible $CO_2$ Capturing from Power Plants. *Energy Convers. Manag.* **2021**, *246*, 114633. [CrossRef]
29. Muhammad, H.A.; Sultan, H.; Lee, B.; Imran, M.; Baek, I.H.; Baik, Y.J.; Nam, S.C. Energy Minimization of Carbon Capture and Storage by Means of a Novel Process Configuration. *Energy Convers. Manag.* **2020**, *215*, 112871. [CrossRef]

30. Merkel, T.C.; Lin, H.; Wei, X.; Baker, R. Power Plant Post-Combustion Carbon Dioxide Capture: An Opportunity for Membranes. *J. Memb. Sci.* **2010**, *359*, 126–139. [CrossRef]
31. Sharma, S.K.; Sanfui, B.K.; Katare, A.; Mandal, B. Fabrication and Performance Evaluation of Industrial Alumina Based Graded Ceramic Substrate for $CO_2$ Selective Amino Silicate Membrane. *ACS Appl. Mater. Interfaces* **2020**, *12*, 40269–40284. [CrossRef] [PubMed]
32. Wang, S.; Li, X.; Wu, H.; Tian, Z.; Xin, Q.; He, G.; Peng, D.; Chen, S.; Yin, Y.; Jiang, Z.; et al. Advances in High Permeability Polymer-Based Membrane Materials for $CO_2$ Separations. *Energy Environ. Sci.* **2016**, *9*, 1863–1890. [CrossRef]
33. Mitchell, J.K. On the Penetrativeness of Fluids. *J. Memb. Sci.* **1995**, *100*, 11–16. [CrossRef]
34. Graham, T. On the Absorption and Dialytic Separation of Gases by Colloid Septa. *J. Frankl. Inst.* **1867**, *83*, 39–41. [CrossRef]
35. Bermeshev, M.V.; Syromolotov, A.V.; Gringolts, M.L.; Starannikova, L.E.; Yampolskii, Y.P.; Finkelshtein, E.S. Synthesis of High Molecular Weight Poly [3-{tris(Trimethylsiloxy)Silyl} Tricyclononenes-7] and Their Gas Permeation Properties. *Macromolecules* **2011**, *44*, 6637–6640. [CrossRef]
36. Vinoba, M.; Bhagiyalakshmi, M.; Alqaheem, Y.; Alomair, A.A.; Pérez, A.; Rana, M.S. Recent Progress of Fillers in Mixed Matrix Membranes for $CO_2$ Separation: A Review. *Sep. Purif. Technol.* **2017**, *188*, 431–450. [CrossRef]
37. Nasir, R.; Mukhtar, H.; Man, Z.; Mohshim, D.F. Material Advancements in Fabrication of Mixed-Matrix Membranes. *Chem. Eng. Technol.* **2013**, *36*, 717–727. [CrossRef]
38. Wong, K.K.; Jawad, Z.A. A Review and Future Prospect of Polymer Blend Mixed Matrix Membrane for $CO_2$ Separation. *J. Polym. Res.* **2019**, *26*, 289. [CrossRef]
39. Kanehashi, S.; Scholes, C.A. Perspective of Mixed Matrix Membranes for Carbon Capture. *Front. Chem. Sci. Eng.* **2020**, *14*, 460–469. [CrossRef]
40. Dong, G.; Li, H.; Chen, V. Challenges and Opportunities for Mixed-Matrix Membranes for Gas Separation. *J. Mater. Chem. A Mater.* **2013**, *1*, 4610–4630. [CrossRef]
41. Suleman, M.S.; Lau, K.K.; Yeong, Y.F. Plasticization and Swelling in Polymeric Membranes in $CO_2$ Removal from Natural Gas. *Chem. Eng. Technol.* **2016**, *39*, 1604–1616. [CrossRef]
42. Arias, A.M.; Mussati, M.C.; Mores, P.L.; Scenna, N.J.; Caballero, J.A.; Mussati, S.F. Optimization of Multi-Stage Membrane Systems for $CO_2$ Capture from Flue Gas. *Int. J. Greenh. Gas. Control* **2016**, *53*, 371–390. [CrossRef]
43. Xu, J.; Wang, Z.; Qiao, Z.; Wu, H.; Dong, S.; Zhao, S.; Wang, J. Post-Combustion $CO_2$ Capture with Membrane Process: Practical Membrane Performance and Appropriate Pressure. *J. Memb. Sci.* **2019**, *581*, 195–213. [CrossRef]
44. Rashid, M.I.; Yaqoob, Z.; Mujtaba, M.A.; Fayaz, H.; Saleel, C.A. Developments in Mineral Carbonation for Carbon Sequestration. *Heliyon* **2023**, *9*, e21796. [CrossRef]
45. Zheng, J.; Chong, Z.R.; Qureshi, M.F.; Linga, P. Carbon Dioxide Sequestration via Gas Hydrates: A Potential Pathway toward Decarbonization. *Energy Fuels* **2020**, *34*, 10529–10546. [CrossRef]
46. Sayani, J.K.S.; Lal, B.; Pedapati, S.R. Comprehensive Review on Various Gas Hydrate Modelling Techniques: Prospects and Challenges. *Arch. Comput. Methods Eng.* **2021**, *29*, 2171–2207. [CrossRef]
47. Sloan, E.D. Fundamental Principles and Applications of Natural Gas Hydrates. *Nature* **2003**, *426*, 353–359. [CrossRef]
48. McMullan, R.K.; Jeffrey, G.A.; McMullan, R.K.; Jeffrey, G.A. Polyhedral Clathrate Hydrates. IX. Structure of Ethylene Oxide Hydrate. *J. Chem. Phys.* **1965**, *42*, 2725–2732. [CrossRef]
49. Mak, T.C.W.; McMullan, R.K.; Mak, T.C.W.; McMullan, R.K. Polyhedral Clathrate Hydrates. X. Structure of the Double Hydrate of Tetrahydrofuran and Hydrogen Sulfide. *J. Chem. Phys.* **1965**, *42*, 2732–2737. [CrossRef]
50. Ripmeester, J.A.; Tse, J.S.; Ratcliffe, C.I.; Powell, B.M.; Ripmeester, J.A.; Tse, J.S.; Ratcliffe, C.I.; Powell, B.M. A New Clathrate Hydrate Structure. *Nature* **1987**, *325*, 135–136. [CrossRef]
51. Sloan, E.D., Jr. Gas Hydrates: Review of Physical/Chemical Properties. *Energy Fuels* **1998**, *12*, 191–196. [CrossRef]
52. Circone, S.; Stern, L.A.; Kirby, S.H.; Durham, W.B.; Chakoumakos, B.C.; Rawn, C.J.; Rondinone, A.J.; Ishii, Y. $CO_2$ Hydrate: Synthesis, Composition, Structure, Dissociation Behavior, and a Comparison to Structure I CH4 Hydrate. *J. Phys. Chem. B* **2003**, *107*, 5529–5539. [CrossRef]
53. Uchida, T. Physical Property Measurements on $CO_2$ Clathrate Hydrates. Review of Crystallography, Hydration Number, and Mechanical Properties. *Waste Manag.* **1998**, *17*, 343–352. [CrossRef]
54. Shimoaka, T.; Hasegawa, T.; Ohno, K.; Katsumoto, Y. Correlation between the Local OH Stretching Vibration Wavenumber and the Hydrogen Bonding Pattern of Water in a Condensed Phase: Quantum Chemical Approach to Analyze the Broad OH Band. *J. Mol. Struct.* **2012**, *1029*, 209–216. [CrossRef]
55. Carey, D.M.; Korenowski, G.M. Measurement of the Raman Spectrum of Liquid Water. *J. Chem. Phys.* **1998**, *108*, 2669–2675. [CrossRef]
56. Giovannetti, R.; Gambelli, A.M.; Castellani, B.; Rossi, A.; Minicucci, M.; Zannotti, M.; Li, Y.; Rossi, F. May Sediments Affect the Inhibiting Properties of NaCl on $CH_4$ and $CO_2$ Hydrates Formation? An Experimental Report. *J. Mol. Liq.* **2022**, *359*, 119300. [CrossRef]

57. Huang, X.; Cai, W.; Zhan, L.; Lu, H. Study on the Reaction of Methane Hydrate with Gaseous $CO_2$ by Raman Imaging Microscopy. *Chem. Eng. Sci.* **2020**, *222*, 115720. [CrossRef]
58. Giovannetti, R.; Gambelli, A.M.; Rossi, A.; Castellani, B.; Minicucci, M.; Zannotti, M.; Nicolini, A.; Rossi, F. Thermodynamic Assessment and Microscale Raman Spectroscopy of Binary $CO_2/CH_4$ Hydrates Produced during Replacement Applications in Natural Reservoirs. *J. Mol. Liq.* **2022**, *368*, 120739. [CrossRef]
59. Falenty, A.; Kuhs, W.F. "Self-Preservation" of $CO_2$ Gas Hydrates-Surface Microstructure and Ice Perfection. *J. Phys. Chem. B* **2009**, *113*, 15975–15988. [CrossRef]
60. Udachin, K.A.; Ratcliffe, C.I.; Ripmeester, J.A. Structure, Composition, and Thermal Expansion of $CO_2$ Hydrate from Single Crystal X-ray Diffraction Measurements. *J. Phys. Chem. B* **2001**, *105*, 4200–4204. [CrossRef]
61. Uchida, T.; Takeya, S.; Wilson, L.D.; Tulk, C.A.; Ripmeester, J.A.; Nagao, J.; Ebinuma, T.; Narita, H. Measurements of Physical Properties of Gas Hydrates and in Situ Observations of Formation and Decomposition Processes via Raman Spectroscopy and X-Ray Diffraction. *Can. J. Phys.* **2003**, *81*, 351–357. [CrossRef]
62. Timur, A. Nuclear Magnetic Resonance Study of Carbonate Rocks. In Proceedings of the SPWLA 13th Annual Logging Symposium, Tulsa, OK, USA, 7–10 May 1972.
63. Ratcliffe, C.I.; Ripmeester, J.A. 1H and 13C NMR Studies on Carbon Dioxide Hydrate. *J. Phys. Chem.* **1986**, *90*, 1259–1263. [CrossRef]
64. Yang, M.; Chong, Z.R.; Zheng, J.; Song, Y.; Linga, P. Advances in Nuclear Magnetic Resonance (NMR) Techniques for the Investigation of Clathrate Hydrates. *Renew. Sustain. Energy Rev.* **2017**, *74*, 1346–1360. [CrossRef]
65. Chevalier, T.; Fleury, M.; Pauget, L.; Sinquin, A. $CO_2$ Hydrate in Porous Media: A Quantitative NMR Method to Detect Formation, Dissociation, and Localization. *Energy Fuels* **2024**, *38*, 22298–22306. [CrossRef]
66. Zheng, J.; Yang, L.; Ma, S.; Zhao, Y.; Yang, M. Quantitative Analysis of $CO_2$ Hydrate Formation in Porous Media by Proton NMR. *AIChE J.* **2020**, *66*, e16820. [CrossRef]
67. Lee, S.; Park, S.; Lee, Y.; Seo, Y. Thermodynamic and 13C NMR Spectroscopic Verification of Methane–Carbon Dioxide Replacement in Natural Gas Hydrates. *Chem. Eng. J.* **2013**, *225*, 636–640. [CrossRef]
68. Dalmazzone, D.; Hamed, N.; Clausse, D.; Fouconnier, B.; Dalmazzone, C.; Herzhaft, B. The Use of DSC in the Study of the Thermodynamics and Kinetics of Formation of Model and Gas Hydrates. In Proceedings of the 5th International Conference on Gas Hydrates (ICGH 2005), Trondheim, Norway, 13–16 June 2005; p. 10.
69. Susilo, R.; Ripmeester, J.A.; Englezos, P. Characterization of Gas Hydrates with PXRD, DSC, NMR, and Raman Spectroscopy. *Chem. Eng. Sci.* **2007**, *62*, 3930–3939. [CrossRef]
70. Lee, Y.; Lee, S.; Lee, J.; Seo, Y. Structure Identification and Dissociation Enthalpy Measurements of the $CO_2$ + $N_2$ Hydrates for Their Application to $CO_2$ Capture and Storage. *Chem. Eng. J.* **2014**, *246*, 20–26. [CrossRef]
71. Handa, Y.P. Compositions, Enthalpies of Dissociation, and Heat Capacities in the Range 85 to 270 K for Clathrate Hydrates of Methane, Ethane, and Propane, and Enthalpy of Dissociation of Isobutane Hydrate, as Determined by a Heat-Flow Calorimeter. *J. Chem. Thermodyn.* **1986**, *18*, 915–921. [CrossRef]
72. Basu, P.K.; Mountain, R.D. Molecular Dynamics Evaluation of Cell Models for Type I Gas Hydrate Crystal Dynamics. *J. Phys. Chem. Solids* **1988**, *49*, 587–588. [CrossRef]
73. Zhang, X.; Yang, H.; Huang, T.; Li, J.; Li, P.; Wu, Q.; Wang, Y.; Zhang, P. Research Progress of Molecular Dynamics Simulation on the Formation-Decomposition Mechanism and Stability of $CO_2$ Hydrate in Porous Media: A Review. *Renew. Sustain. Energy Rev.* **2022**, *167*, 112820. [CrossRef]
74. Li, H.; Jakobsen, J.P.; Stang, J. Hydrate Formation during $CO_2$ Transport: Predicting Water Content in the Fluid Phase in Equilibrium with the $CO_2$-Hydrate. *Int. J. Greenh. Gas. Control* **2011**, *5*, 549–554. [CrossRef]
75. Bollengier, O.; Choukroun, M.; Grasset, O.; Le Menn, E.L.; Bellino, G.; Morizet, Y.; Bezacier, L.; Oancea, A.; Taffin, C.; Tobie, G. Phase Equilibria in the $H_2O$–$CO_2$ System between 250–330 K and 0–1.7 GPa: Stability of the $CO_2$ Hydrates and $H_2O$-Ice VI at $CO_2$ Saturation. *Geochim. Cosmochim. Acta* **2013**, *119*, 322–339. [CrossRef]
76. Sloan, E.D., Jr.; Koh, C.A.; Koh, C.A. *Clathrate Hydrates of Natural Gases*; CRC Press: Boca Raton, FL, USA, 2007. [CrossRef]
77. Smith, J.; Van Ness, H.; Abott, M. *Introduction to Chemical Engineering Thermodynamics*, 6th ed.; McGraw-Hill: New York, NY, USA, 2001.
78. Schicks, J.M. Gas Hydrates in Nature and in the Laboratory: Necessary Requirements for Formation and Properties of the Resulting Hydrate Phase. *ChemTexts* **2022**, *8*, 13. [CrossRef]
79. Radhakrishnan, R.; Trout, B.L. A New Approach for Studying Nucleation Phenomena Using Molecular Simulations: Application to $CO_2$ Hydrate Clathrates. *J. Chem. Phys.* **2002**, *117*, 1786–1796. [CrossRef]
80. Jacobson, L.C.; Hujo, W.; Molinero, V. Amorphous Precursors in the Nucleation of Clathrate Hydrates. *J. Am. Chem. Soc.* **2010**, *132*, 11806–11811. [CrossRef]
81. Yang, S.O.; Yang, I.M.; Kim, Y.S.; Lee, C.S. Measurement and Prediction of Phase Equilibria for Water+$CO_2$ in Hydrate Forming Conditions. *Fluid. Phase Equilib.* **2000**, *175*, 75–89. [CrossRef]

82. Ke, W.; Svartaas, T.M.; Chen, D. A Review of Gas Hydrate Nucleation Theories and Growth Models. *J. Nat. Gas. Sci. Eng.* **2019**, *61*, 169–196. [CrossRef]
83. Kvamme, B.; Baig, K.; Qasim, M.; Bauman, J. Thermodynamic and Kinetic Modeling of $CH_4/CO_2$ Hydrates Phase Transitions. *Int. J. Energy Environ.* **2013**, *7*, 1–8.
84. Koh, C.A.; Sloan, E.D.; Sum, A.K.; Wu, D.T. Fundamentals and Applications of Gas Hydrates. *Annu. Rev. Chem. Biomol. Eng.* **2011**, *2*, 237–257. [CrossRef] [PubMed]
85. Maeda, N. Interfacial Gaseous States. In *Nucleation of Gas Hydrates*; Springer: Cham, Switzerland, 2020; pp. 83–109. [CrossRef]
86. Seo, Y.; Lee, H.; Uchida, T. Methane and Carbon Dioxide Hydrate Phase Behavior in Small Porous Silica Gels: Three-Phase Equilibrium Determination and Thermodynamic Modeling. *Langmuir* **2002**, *18*, 9164–9170. [CrossRef]
87. Gambelli, A.M.; Rossi, F. Experimental Characterization of the Difference in Induction Period between $CH_4$ and $CO_2$ Hydrates: Motivations and Possible Consequences on the Replacement Process. *J. Nat. Gas. Sci. Eng.* **2022**, *108*, 104848. [CrossRef]
88. Lv, X.; Lu, D.; Liu, Y.; Zhou, S.; Zuo, J.; Jin, H.; Shi, B.; Li, E. Study on Methane Hydrate Formation in Gas–Water Systems with a New Compound Promoter. *RSC Adv.* **2019**, *9*, 33506–33518. [CrossRef] [PubMed]
89. Babu, P.; Kumar, R.; Linga, P. A New Porous Material to Enhance the Kinetics of Clathrate Process: Application to Precombustion Carbon Dioxide Capture. *Environ. Sci. Technol.* **2013**, *47*, 13191–13198. [CrossRef] [PubMed]
90. Yang, M.; Song, Y.; Jiang, L.; Wang, X.; Liu, W.; Zhao, Y.; Liu, Y.; Wang, S. Dynamic Measurements of Hydrate Based Gas Separation in Cooled Silica Gel. *J. Ind. Eng. Chem.* **2014**, *20*, 322–330. [CrossRef]
91. Li, A.; Jiang, L.; Tang, S. An Experimental Study on Carbon Dioxide Hydrate Formation Using a Gas-Inducing Agitated Reactor. *Energy* **2017**, *134*, 629–637. [CrossRef]
92. Bhavya, T.; Sai Kiran, B.; Prasad, P.S.R. The Role of Stirring and Amino Acid Mixtures to Surpass the Sluggishness of $CO_2$ Hydrates. *Energy Fuels* **2021**, *35*, 13937–13944. [CrossRef]
93. Sun, Y.; Li, K.; Su, Y.; Zhao, J. Phase Diagrams for SII Clathrate Hydrates of $CO_2$ from First-Principles Thermodynamics. *J. Phys. Chem. A* **2021**, *125*, 5956–5962. [CrossRef]
94. He, Z.; Praveen, L.; Jianwen, J. What Are the Key Factors Governing the Nucleation of $CO_2$ Hydrate? *Phys. Chem. Chem. Phys.* **2017**, *19*, 15657–15661. [CrossRef]
95. English, N.J.; MacElroy, J.M.D. Perspectives on Molecular Simulation of Clathrate Hydrates: Progress, Prospects and Challenges. *Chem. Eng. Sci.* **2015**, *121*, 133–156. [CrossRef]
96. Lee, Y.; Kim, H.; Lee, W.; Kang, D.W.; Lee, J.W.; Ahn, Y.H. Thermodynamic and Kinetic Properties of $CO_2$ Hydrates and Their Applications in $CO_2$ Capture and Separation. *J. Environ. Chem. Eng.* **2023**, *11*, 110933. [CrossRef]
97. Dubey, A.; Arora, A. Effect of Promoters in Hydrates Based Carbon Dioxide Capture: A Review. *Gas. Sci. Eng.* **2024**, *131*, 205459. [CrossRef]
98. Veluswamy, H.P.; Kumar, A.; Seo, Y.; Lee, J.D.; Linga, P. A Review of Solidified Natural Gas (SNG) Technology for Gas Storage via Clathrate Hydrates. *Appl. Energy* **2018**, *216*, 262–285. [CrossRef]
99. Kimura, H.; Kai, J. Feasibility of Trichlorofluoromethane (CCl3F, R11) Heptadecahydrate as a Heat Storage Material. *Energy Convers. Manag.* **1985**, *25*, 179–186. [CrossRef]
100. Molokitina, N.S.; Nesterov, A.N.; Podenko, L.S.; Reshetnikov, A.M. Carbon Dioxide Hydrate Formation with SDS: Further Insights into Mechanism of Gas Hydrate Growth in the Presence of Surfactant. *Fuel* **2019**, *235*, 1400–1411. [CrossRef]
101. Watanabe, K.; Imai, S.; Mori, Y.H. Surfactant Effects on Hydrate Formation in an Unstirred Gas/Liquid System: An Experimental Study Using HFC-32 and Sodium Dodecyl Sulfate. *Chem. Eng. Sci.* **2005**, *60*, 4846–4857. [CrossRef]
102. Asaoka, T.; Ikeda, K. Observation of the Growth Characteristics of Gas Hydrate in the Quiescent-Type Formation Method Using Surfactant. *J. Cryst. Growth* **2017**, *478*, 1–8. [CrossRef]
103. Kumar, A.; Sakpal, T.; Linga, P.; Kumar, R. Influence of Contact Medium and Surfactants on Carbon Dioxide Clathrate Hydrate Kinetics. *Fuel* **2013**, *105*, 664–671. [CrossRef]
104. Choi, J.W.; Chung, J.T.; Kang, Y.T. $CO_2$ Hydrate Formation at Atmospheric Pressure Using High Efficiency Absorbent and Surfactants. *Energy* **2014**, *78*, 869–876. [CrossRef]
105. Wang, F.; Guo, G.; Liu, G.Q.; Luo, S.J.; Guo, R.B. Effects of Surfactant Micelles and Surfactant-Coated Nanospheres on Methane Hydrate Growth Pattern. *Chem. Eng. Sci.* **2016**, *144*, 108–115. [CrossRef]
106. Karaaslan, U.; Parlaktuna, M. Surfactants as Hydrate Promoters? *Energy Fuels* **2000**, *14*, 1103–1107. [CrossRef]
107. Sun, Z.; Wang, R.; Ma, R.; Guo, K.; Fan, S. Effect of Surfactants and Liquid Hydrocarbons on Gas Hydrate Formation Rate and Storage Capacity. *Int. J. Energy Res.* **2003**, *27*, 747–756. [CrossRef]
108. Ganji, H.; Manteghian, M.; Zadeh, K.S.; Omidkhah, M.R.; Rahimi Mofrad, H. Effect of Different Surfactants on Methane Hydrate Formation Rate, Stability and Storage Capacity. *Fuel* **2007**, *86*, 434–441. [CrossRef]
109. Yuan, B.; Han, M.; Li, Y.; Liu, X.; Kang, L.; Tong, X.; Wang, P.; Han, S.; Zhu, J.; Zhao, Y.; et al. Roles of Short- and Long-Chain Organic Matter in Methane Hydrate Formation: Insights from Molecular Dynamics Simulations. *Energy Fuels* **2024**, *38*, 9742–9750. [CrossRef]

110. Yoslim, J.; Linga, P.; Englezos, P. Enhanced Growth of Methane–Propane Clathrate Hydrate Crystals with Sodium Dodecyl Sulfate, Sodium Tetradecyl Sulfate, and Sodium Hexadecyl Sulfate Surfactants. *J. Cryst. Growth* **2010**, *313*, 68–80. [CrossRef]
111. Okutani, K.; Kuwabara, Y.; Mori, Y.H. Surfactant Effects on Hydrate Formation in an Unstirred Gas/Liquid System: An Experimental Study Using Methane and Sodium Alkyl Sulfates. *Chem. Eng. Sci.* **2008**, *63*, 183–194. [CrossRef]
112. Zeng, H.; Wilson, L.D.; Walker, V.K.; Ripmeester, J.A. Effect of Antifreeze Proteins on the Nucleation, Growth, and the Memory Effect during Tetrahydrofuran Clathrate Hydrate Formation. *J. Am. Chem. Soc.* **2006**, *128*, 2844–2850. [CrossRef]
113. Dicharry, C.; Diaz, J.; Torré, J.P.; Ricaurte, M. Influence of the Carbon Chain Length of a Sulfate-Based Surfactant on the Formation of $CO_2$, $CH_4$ and $CO_2$–$CH_4$ Gas Hydrates. *Chem. Eng. Sci.* **2016**, *152*, 736–745. [CrossRef]
114. Delahaye, A.; Fournaison, L.; Marinhas, S.; Chatti, I.; Petitet, J.P.; Dalmazzone, D.; Fürst, W. Effect of THF on Equilibrium Pressure and Dissociation Enthalpy of $CO_2$ Hydrates Applied to Secondary Refrigeration. *Ind. Eng. Chem. Res.* **2005**, *45*, 391–397. [CrossRef]
115. Bhawangirkar, D.R.; Liu, X.; Sun, B.; Zhao, J.; Yin, Z. Tuning Effect of THF on the Phase Equilibria, Storage Capacity, and Dissociation Heat of $CO_2$ Hydrates: Implication for Hydrate-Based $CO_2$ Sequestration. *Fuel* **2025**, *396*, 135293. [CrossRef]
116. Ricaurte, M.; Dicharry, C.; Renaud, X.; Torré, J.P. Combination of Surfactants and Organic Compounds for Boosting $CO_2$ Separation from Natural Gas by Clathrate Hydrate Formation. *Fuel* **2014**, *122*, 206–217. [CrossRef]
117. Phan, A.; Striolo, A. Chemical Promoter Performance for $CO_2$ Hydrate Growth: A Molecular Perspective. *Energy Fuels* **2023**, *37*, 6002–6011. [CrossRef]
118. Sharma, R.; Kamal, A.; Abdinejad, M.; Mahajan, R.K.; Kraatz, H.B. Advances in the Synthesis, Molecular Architectures and Potential Applications of Gemini Surfactants. *Adv. Colloid Interface Sci.* **2017**, *248*, 35–68. [CrossRef] [PubMed]
119. He, Y.; Sun, M.T.; Chen, C.; Zhang, G.D.; Chao, K.; Lin, Y.; Wang, F. Surfactant-Based Promotion to Gas Hydrate Formation for Energy Storage. *J. Mater. Chem. A Mater.* **2019**, *7*, 21634–21661. [CrossRef]
120. Ndlovu, P.; Babaee, S.; Naidoo, P.; Moodley, K. Kinetic Studies of Gas Hydrates for $CO_2$ Capture in the Presence of Nanoparticles. *Ind. Eng. Chem. Res.* **2024**, *63*, 3867–3879. [CrossRef]
121. Wang, L.; Lu, X.; Xu, Y. Experiment Investigation of $SiO_2$ Containing Amino Groups as a Kinetic Promoter for $CO_2$ Hydrates. *ACS Omega* **2021**, *6*, 19748–19756. [CrossRef]
122. Khanlarkhani, M.; Pahlavanzadeh, H.; Mohammadi, A.H.; Mohammadi, A.H. Clathrate Hydrates and Nano Particles. *Nanotechnol. Res. J.* **2015**, *8*, 149–162.
123. Wu, Y.; Shang, L.; Pan, Z.; Xuan, Y.; Baena-Moreno, F.M.; Zhang, Z. Gas Hydrate Formation in the Presence of Mixed Surfactants and Alumina Nanoparticles. *J. Nat. Gas Sci. Eng.* **2021**, *94*, 104049. [CrossRef]
124. Nesterov, A.N.; Reshetnikov, A.M.; Manakov, A.Y.; Adamova, T.P. Synergistic Effect of Combination of Surfactant and Oxide Powder on Enhancement of Gas Hydrates Nucleation. *J. Energy Chem.* **2017**, *26*, 808–814. [CrossRef]
125. Mohammadi, A.; Manteghian, M.; Mohammadi, A.H.; Jahangiri, A. Induction Time, Storage Capacity, and Rate of Methane Hydrate Formation in the Presence of SDS and Silver Nanoparticles. *Chem. Eng. Commun.* **2017**, *204*, 1420–1427. [CrossRef]
126. Mohammadi, A.; Manteghian, M.; Haghtalab, A.; Mohammadi, A.H.; Rahmati-Abkenar, M. Kinetic Study of Carbon Dioxide Hydrate Formation in Presence of Silver Nanoparticles and SDS. *Chem. Eng. J.* **2014**, *237*, 387–395. [CrossRef]
127. Nashed, O.; Youssouf, S.M.; Sabil, K.M.; Shariff, A.M.; Sufian, S.; Lal, B. Investigating the Effect of Silver Nanoparticles on Carbon Dioxide Hydrates Formation. In *Proceedings of the IOP Conference Series: Materials Science and Engineering*; Institute of Physics Publishing: Bristol, UK, 2018; Volume 458.
128. Mahmoodi, M.H.; Manteghian, M.; Naeiji, P. Study the Effect of Ag Nanoparticles on the Kinetics of $CO_2$ Hydrate Growth by Molecular Dynamics Simulation. *J. Mol. Liq.* **2021**, *343*, 117668. [CrossRef]
129. Hassan, H.; Javidani, A.M.; Mohammadi, A.; Pahlavanzadeh, H.; Abedi-Farizhendi, S.; Mohammadi, A.H. Effects of Graphene Oxide Nanosheets and $Al_2O_3$ Nanoparticles on $CO_2$ Uptake in Semi-Clathrate Hydrates. *Chem. Eng. Technol.* **2021**, *44*, 48–57. [CrossRef]
130. Zhou, S.D.; Yu, Y.S.; Zhao, M.M.; Wang, S.L.; Zhang, G.Z. Effect of Graphite Nanoparticles on Promoting $CO_2$ Hydrate Formation. *Energy Fuels* **2014**, *28*, 4694–4698. [CrossRef]
131. Mahant, B.; Patel, D.; Kushwaha, O.S.; Kumar, R. Systematic Study of Nanohybrids of ZnO Nanoparticles toward Enhancement of Gas Hydrate Kinetics and the Application in Energy Storage. *Energy Fuels* **2023**, *37*, 19621–19638. [CrossRef]
132. Mousavi, S.E.; Bozorgian, A. Investigation the Kinetics of $CO_2$ Hydrate Formation in the Water System + CTAB + TBAF + ZnO. *Int. J. New Chem.* **2020**, *7*, 195–219. [CrossRef]
133. Pahlavanzadeh, H.; Ataie, P.; Eslamimanesh, A. Phase Equilibria of Zinc Oxide (ZnO) Nanoparticles and Tetrahydrofuran (THF) in $CO_2$ Hydrate Systems: Individual and Combined Analyses. *J. Chem. Eng. Data* **2024**, *69*, 3055–3062. [CrossRef]
134. Rajabi Firoozabadi, S.; Bonyadi, M. A Comparative Study on the Effects of $Fe_3O_4$ Nanofluid, SDS and CTAB Aqueous Solutions on the $CO_2$ Hydrate Formation. *J. Mol. Liq.* **2020**, *300*, 112251. [CrossRef]
135. Cheng, Z.; Xu, H.; Wang, S.; Liu, W.; Li, Y.; Jiang, L.; Chen, C.; Song, Y. Effect of Nanoparticles as a Substitute for Kinetic Additives on the Hydrate-Based $CO_2$ Capture. *Chem. Eng. J.* **2021**, *424*, 130329. [CrossRef]

136. Sowa, B.; Maeda, N. Statistical Study of the Memory Effect in Model Natural Gas Hydrate Systems. *J. Phys. Chem. A* **2015**, *119*, 10784–10790. [CrossRef]
137. Takeya, S.; Hori, A.; Hondoh, T.; Uchida, T. Freezing-Memory Effect of Water on Nucleation of $CO_2$ Hydrate Crystals. *J. Phys. Chem. B* **2000**, *104*, 4164–4168. [CrossRef]
138. Wu, Q.; Zhang, B. Memory Effect on the Pressure-Temperature Condition and Induction Time of Gas Hydrate Nucleation. *J. Nat. Gas Chem.* **2010**, *19*, 446–451. [CrossRef]
139. Sefidroodi, H.; Abrahamsen, E.; Kelland, M.A. Investigation into the Strength and Source of the Memory Effect for Cyclopentane Hydrate. *Chem. Eng. Sci.* **2013**, *87*, 133–140. [CrossRef]
140. He, Y.; Rudolph, E.S.J.; Zitha, P.L.J.; Golombok, M. Kinetics of $CO_2$ and Methane Hydrate Formation: An Experimental Analysis in the Bulk Phase. *Fuel* **2011**, *90*, 272–279. [CrossRef]
141. Sloan, E.D.; Subramanian, S.; Matthews, P.N.; Lederhos, J.P.; Khokhar, A.A. Quantifying Hydrate Formation and Kinetic Inhibition. *Ind. Eng. Chem. Res.* **1998**, *37*, 3124–3132. [CrossRef]
142. Ohmura, R.; Ogawa, M.; Yasuoka, K.; Mori, Y.H. Statistical Study of Clathrate-Hydrate Nucleation in a Water/Hydrochlorofluorocarbon System: Search for the Nature of the "Memory Effect". *J. Phys. Chem. B* **2003**, *107*, 5289–5293. [CrossRef]
143. Kuang, Y.; Li, W.; Lin, Z.; Zheng, Y.; Craig, V.S.J. Experimental Study on Memory Effect of Gas Hydrates: Interaction between Micronanobubbles and Solute Molecules. *J. Phys. Chem. C* **2024**, *128*, 13. [CrossRef]
144. Ripmeester, J.A.; Alavi, S. Some Current Challenges in Clathrate Hydrate Science: Nucleation, Decomposition and the Memory Effect. *Curr. Opin. Solid. State Mater. Sci.* **2016**, *20*, 344–351. [CrossRef]
145. Maeda, N. Interfacial Nanobubbles and the Memory Effect of Natural Gas Hydrates. *J. Phys. Chem. C* **2018**, *122*, 11399–11406. [CrossRef]
146. Aghajanloo, M.; Yan, L.; Berg, S.; Voskov, D.; Farajzadeh, R. Impact of $CO_2$ Hydrates on Injectivity during $CO_2$ Storage in Depleted Gas Fields: A Literature Review. *Gas. Sci. Eng.* **2024**, *123*, 205250. [CrossRef]
147. Gauteplass, J.; Almenningen, S.; Barth, T.; Ersland, G. Hydrate Plugging and Flow Remediation during $CO_2$ Injection in Sediments. *Energies* **2020**, *13*, 4511. [CrossRef]
148. Chong, Z.R.; Yang, S.H.B.; Babu, P.; Linga, P.; Li, X. Sen Review of Natural Gas Hydrates as an Energy Resource: Prospects and Challenges. *Appl. Energy* **2016**, *162*, 1633–1652. [CrossRef]
149. McGrail, B.P.; Schaef, H.T.; White, M.D.; Zhu, T.; Kulkarni, A.S.; Hunter, R.B.; Patil, S.L.; Owen, A.T.; Martin, P.F. *Using Carbon Dioxide to Enhance Recovery of Methane from Gas Hydrate Reservoirs: Final Summary Report*; Pacific Northwest National Lab. (PNNL): Richland, WA, USA, 2007. [CrossRef]
150. Cannone, S.F.; Lanzini, A.; Santarelli, M. A Review on $CO_2$ Capture Technologies with Focus on $CO_2$-Enhanced Methane Recovery from Hydrates. *Energies* **2021**, *14*, 387. [CrossRef]
151. Park, Y.; Kim, D.Y.; Lee, J.W.; Huh, D.G.; Park, K.P.; Lee, J.; Lee, H. Sequestering Carbon Dioxide into Complex Structures of Naturally Occurring Gas Hydrates. *Proc. Natl. Acad. Sci. USA* **2006**, *103*, 12690–12694. [CrossRef]
152. Lee, S.; Lee, Y.; Lee, J.; Lee, H.; Seo, Y. Experimental Verification of Methane-Carbon Dioxide Replacement in Natural Gas Hydrates Using a Differential Scanning Calorimeter. *Environ. Sci. Technol.* **2013**, *47*, 13184–13190. [CrossRef]
153. Schicks, J.M.; Luzi, M.; Beeskow-Strauch, B. The Conversion Process of Hydrocarbon Hydrates into $CO_2$ Hydrates and Vice Versa: Thermodynamic Considerations. *J. Phys. Chem. A* **2011**, *115*, 13324–13331. [CrossRef]
154. Ota, M.; Abe, Y.; Watanabe, M.; Smith, R.L.; Inomata, H. Methane Recovery from Methane Hydrate Using Pressurized $CO_2$. *Fluid Phase Equilib.* **2005**, *228–229*, 553–559. [CrossRef]
155. Zhong, J.R.; Huang, K.B.; Yang, S.; Luo, Z.Z.; Zhu, Y.X.; Wan, L.; Sun, Y.F.; Sun, C.Y.; Chen, G.J.; Zhang, Y.F. Quantifying the Limits of $CH_4$-$CO_2$ Hydrate Replacement: Impact of Critical Replacement Thickness, Particle Size, and Flow Rate on Recovery Efficiency. *Energy Fuels* **2025**, *39*, 5741–5753. [CrossRef]
156. Ruppel, C.D.; Kessler, J.D. The Interaction of Climate Change and Methane Hydrates. *Rev. Geophys.* **2017**, *55*, 126–168. [CrossRef]
157. Falenty, A.; Qin, J.; Salamatin, A.N.; Yang, L.; Kuhs, W.F. Fluid Composition and Kinetics of the in Situ Replacement in $CH_4$–$CO_2$ Hydrate System. *J. Phys. Chem. C* **2016**, *120*, 27159–27172. [CrossRef]
158. Pandey, J.S.; Karantonidis, C.; Karcz, A.P.; von Solms, N. Enhanced $CH_4$-$CO_2$ Hydrate Swapping in the Presence of Low Dosage Methanol. *Energies* **2020**, *13*, 5238. [CrossRef]
159. Baig, K.; Kvamme, B.; Kuznetsova, T.; Bauman, J. Impact of Water Film Thickness on Kinetic Rate of Mixed Hydrate Formation during Injection of $CO_2$ into $CH_4$ Hydrate. *AIChE J.* **2015**, *61*, 3944–3957. [CrossRef]
160. Ripmeester, J.A.; Ratcliffe, C.I. The Diverse Nature of Dodecahedral Cages in Clathrate Hydrates as Revealed by 129Xe and 13C NMR Spectroscopy: $CO_2$ as a Small-Cage Guest. *Energy Fuels* **1998**, *12*, 197–200. [CrossRef]
161. Salamatin, A.N.; Falenty, A.; Hansen, T.C.; Kuhs, W.F. Guest Migration Revealed in $CO_2$ Clathrate Hydrates. *Energy Fuels* **2015**, *29*, 5681–5691. [CrossRef]

162. Xie, Y.; Zhu, Y.J.; Zheng, T.; Yuan, Q.; Sun, C.Y.; Yang, L.Y.; Chen, G.J. Replacement in $CH_4$-$CO_2$ Hydrate below Freezing Point Based on Abnormal Self-Preservation Differences of $CH_4$ Hydrate. *Chem. Eng. J.* **2021**, *403*, 126283. [CrossRef]
163. Salamatin, A.N.; Falenty, A.; Kuhs, W.F. Diffusion Model for Gas Replacement in an Isostructural $CH_4$-$CO_2$ Hydrate System. *J. Phys. Chem. C* **2017**, *121*, 17603–17616. [CrossRef]
164. Lee, H.; Seo, Y.; Seo, Y.T.; Moudrakovski, I.L.; Ripmeester, J.A. Recovering Methane from Solid Methane Hydrate with Carbon Dioxide. *Angew. Chem. Int. Ed.* **2003**, *42*, 5048–5051. [CrossRef]
165. Koh, D.Y.; Kang, H.; Kim, D.O.; Park, J.; Cha, M.; Lee, H. Recovery of Methane from Gas Hydrates Intercalated within Natural Sediments Using $CO_2$ and a $CO_2$/N2 Gas Mixture. *ChemSusChem* **2012**, *5*, 1443–1448. [CrossRef]
166. Yao, Y.; Niu, M.; Zi, M.; Chen, D. Thermodynamic Stability and Component Heterogeneity of $CO_2$/$N_2$ Mixed Hydrates: Implications for Hydrate-Based $CO_2$ Capture and Sequestration. *Sep. Purif. Technol.* **2025**, *357*, 130151. [CrossRef]
167. Mok, J.; Kim, S.; Lee, J.; Choi, W.; Seo, Y. Investigating the Impact of $N_2$ Concentration on Ternary Gas Hydrate Formation for $CH_4$ Production and $CO_2$ Storage. *J. Mol. Liq.* **2025**, *429*, 127578. [CrossRef]
168. Yousif, M.H. Effect of Underinhibition With Methanol and Ethylene Glycol on the Hydrate-Control Process. *SPE Prod. Facil.* **1998**, *13*, 184–189. [CrossRef]
169. Nihous, G.C.; Kinoshita, C.K.; Masutani, S.M. A Determination of the Activity of Water in Water–Alcohol Mixtures Using Mobile Order Thermodynamics. *Chem. Eng. Sci.* **2009**, *64*, 2767–2771. [CrossRef]
170. Avula, V.R.; Gardas, R.L.; Sangwai, J.S. An Efficient Model for the Prediction of $CO_2$ Hydrate Phase Stability Conditions in the Presence of Inhibitors and Their Mixtures. *J. Chem. Thermodyn.* **2015**, *85*, 163–170. [CrossRef]
171. Bozorgian, A. Investigation of Hydrate Formation Kinetics and Mechanism of Effect of Inhibitors on It, a Review. *J. Chem. Rev.* **2021**, *3*, 50–65.
172. Vatani, Z.; Amini, G.; Samadi, M.; Fuladgar, A.M. Prediction of Gas Hydrate Formation in the Presence of Methanol, Ethanol, (Ethylene, Diethylene and Triethylene) Glycol Thermodynamic Inhibitors. *Pet. Sci. Technol.* **2018**, *36*, 1150–1157. [CrossRef]
173. Abay, H.K.; Svartaas, T.M. Effect of Ultralow Concentration of Methanol on Methane Hydrate Formation. *Energy Fuels* **2010**, *24*, 752–757. [CrossRef]
174. Mokhatab, S.; Wilkens, R.J.; Leontaritis, K.J. A Review of Strategies for Solving Gas-Hydrate Problems in Subsea Pipelines. *Energy Sources Part. A Recovery Util. Environ. Eff.* **2007**, *29*, 39–45. [CrossRef]
175. Khurana, M.; Yin, Z.; Linga, P. A Review of Clathrate Hydrate Nucleation. *ACS Sustain. Chem. Eng.* **2017**, *5*, 11176–11203. [CrossRef]
176. Nguyen, N.N.; Nguyen, A.V. Hydrophobic Effect on Gas Hydrate Formation in the Presence of Additives. *Energy Fuels* **2017**, *31*, 10311–10323. [CrossRef]
177. Lederhos, J.P.; Long, J.P.; Sum, A.; Christiansen, R.L.; Sloan, E.D. Effective Kinetic Inhibitors for Natural Gas Hydrates. *Chem. Eng. Sci.* **1996**, *51*, 1221–1229. [CrossRef]
178. Yagasaki, T.; Matsumoto, M.; Tanaka, H. Adsorption Mechanism of Inhibitor and Guest Molecules on the Surface of Gas Hydrates. *J. Am. Chem. Soc.* **2015**, *137*, 12079–12085. [CrossRef] [PubMed]
179. Moon, C.; Hawtin, R.W.; Rodger, P.M. Nucleation and Control of Clathrate Hydrates: Insights from Simulation. *Faraday Discuss.* **2007**, *136*, 367–382. [CrossRef]
180. Chi Fai Cheung, R.; Bun Ng, T.; Ho Wong, J. Antifreeze Proteins from Diverse Organisms and Their Applications: An Overview. *Curr. Protein Pept. Sci.* **2016**, *18*, 262–283. [CrossRef] [PubMed]
181. Clomp, U.C.; Kruka, V.R.; Reijnhart, R.; Weisenborn, A.J. Method for Inhibiting the Plugging of Conduits by Gas Hydrates. U.S. Patent 5,648,575, 15 July 1997.
182. Bourgmayer, A.; Sugier, A.; Behar, E. *4th Multiphase FlowConference*; BHR Group: Nice, France, 1989.
183. Chen, H.N.; Sun, Y.F.; Pang, W.X.; Wang, M.L.; Wang, M.; Zhong, J.R.; Ren, L.L.; Cao, B.J.; Rao, D.; Sun, C.Y.; et al. Quantitative Evaluation of Hydrate-Based $CO_2$ Storage in Unsealed Marine Sediments: Viewpoint from the Driving Force of Hydrate Formation and $CO_2$-Water Contact Ability. *Fuel* **2024**, *376*, 132682. [CrossRef]
184. Terzariol, M.; Park, J.; Castro, G.M.; Santamarina, J.C. Methane Hydrate-Bearing Sediments: Pore Habit and Implications. *Mar. Pet. Geol.* **2020**, *116*, 104302. [CrossRef]
185. Ruppel, C. Permafrost-Associated Gas Hydrate: Is It Really Approximately 1% of the Global System? *J. Chem. Eng. Data* **2015**, *60*, 429–436. [CrossRef]
186. Zhang, Z.; Liu, L.; Lu, W.; Liu, C.; Ning, F.; Dai, S. Permeability of Hydrate-Bearing Fine-Grained Sediments: Research Status, Challenges and Perspectives. *Earth Sci. Rev.* **2023**, *244*, 104517. [CrossRef]
187. Wu, P.; Li, Y.; Wang, L.; Sun, X.; Wu, D.; He, Y.; Li, Q.; Song, Y. Hydrate-Bearing Sediment of the South China Sea: Microstructure and Mechanical Characteristics. *Eng. Geol.* **2022**, *307*, 106782. [CrossRef]
188. Liang, Y.; Tan, Y.; Luo, Y.; Zhang, Y.; Li, B. Progress and Challenges on Gas Production from Natural Gas Hydrate-Bearing Sediment. *J. Clean. Prod.* **2020**, *261*, 121061. [CrossRef]

189. Yoneda, J.; Jin, Y.; Muraoka, M.; Oshima, M.; Suzuki, K.; Walker, M.; Otsuki, S.; Kumagai, K.; Collett, T.S.; Boswell, R.; et al. Multiple Physical Properties of Gas Hydrate-Bearing Sediments Recovered from Alaska North Slope 2018 Hydrate-01 Stratigraphic Test Well. *Mar. Pet. Geol.* **2021**, *123*, 104748. [CrossRef]
190. Liu, H.; Wang, S.; Fu, Y.; Shi, C.; Song, Y.; Zhang, L.; Chen, C.; Yang, M.; Ling, Z. The Role of Clay in Hydrate-Based Carbon Emission Reduction: Phenomenon, Mechanisms, and Application. *Fuel* **2025**, *389*, 134575. [CrossRef]
191. Vasheghani Farahani, M.; Hassanpouryouzband, A.; Yang, J.; Tohidi, B. Insights into the Climate-Driven Evolution of Gas Hydrate-Bearing Permafrost Sediments: Implications for Prediction of Environmental Impacts and Security of Energy in Cold Regions. *RSC Adv.* **2021**, *11*, 14334–14346. [CrossRef] [PubMed]
192. Jiang, L.; Yu, M.; Liu, Y.; Yang, M.; Zhang, Y.; Xue, Z.; Suekane, T.; Song, Y. Behavior of $CO_2$/Water Flow in Porous Media for $CO_2$ Geological Storage. *Magn. Reson. Imaging* **2017**, *37*, 100–106. [CrossRef] [PubMed]
193. Merey, S.; Al-Raoush, R.I.; Jung, J.; Alshibli, K.A. Comprehensive Literature Review on $CH_4$-$CO_2$ Replacement in Microscale Porous Media. *J. Pet. Sci. Eng.* **2018**, *171*, 48–62. [CrossRef]
194. Ors, O.; Sinayuc, C. An Experimental Study on the $CO_2$–CH4 Swap Process between Gaseous $CO_2$ and $CH_4$ Hydrate in Porous Media. *J. Pet. Sci. Eng.* **2014**, *119*, 156–162. [CrossRef]
195. Wang, P.; Yang, M.; Chen, B.; Zhao, Y.; Zhao, J.; Song, Y. Methane Hydrate Reformation in Porous Media with Methane Migration. *Chem. Eng. Sci.* **2017**, *168*, 344–351. [CrossRef]
196. Zhao, J.; Zhu, Z.; Song, Y.; Liu, W.; Zhang, Y.; Wang, D. Analyzing the Process of Gas Production for Natural Gas Hydrate Using Depressurization. *Appl. Energy* **2015**, *142*, 125–134. [CrossRef]
197. Nair, V.C.; Ramesh, S.; Ramadass, G.A.; Sangwai, J.S. Influence of Thermal Stimulation on the Methane Hydrate Dissociation in Porous Media under Confined Reservoir. *J. Pet. Sci. Eng.* **2016**, *147*, 547–559. [CrossRef]
198. Langevin, D.; Baudin, F.; Henaut, I.; Pasquier, D.; Rovinetti, S.; Espagne, B.; Zhang, P.; Wang, Y.; Yang, Y.; Chen, W.; et al. Methane Hydrate Formation and Dissociation in the Presence of Silica Sand and Bentonite Clay. *Oil Gas. Sci. Technol.—Rev. D'ifp Energ. Nouv.* **2015**, *70*, 1087–1099. [CrossRef]
199. Aman, Z.M.; Boswell, R.; Anderson, R.; Pandey, M.R.; Priest, J.A.; Hayley, J.L. The Influence of Particle Size and Hydrate Formation Path on the Geomechanical Behavior of Hydrate Bearing Sands. *Energies* **2022**, *15*, 9632. [CrossRef]
200. Zang, X.Y.; Liang, D.Q.; Wu, N.Y. Gas Hydrate Formation in Fine Sand. *Sci. China Earth Sci.* **2013**, *56*, 549–556. [CrossRef]
201. Huang, R.; Zhao, Y.; Ma, Y.; Huang, R.; Zhao, Y.; Ma, Y. The Interaction of Talc, Montmorillonite, and Silica Sand with $H_2O$ Influences Methane Hydrate Formation. *Energies* **2023**, *16*, 6174. [CrossRef]
202. Mekala, P.; Busch, M.; Mech, D.; Patel, R.S.; Sangwai, J.S. Effect of Silica Sand Size on the Formation Kinetics of $CO_2$ Hydrate in Porous Media in the Presence of Pure Water and Seawater Relevant for $CO_2$ Sequestration. *J. Pet. Sci. Eng.* **2014**, *122*, 1–9. [CrossRef]
203. Pan, M.; Schicks, J.M. Unraveling the Role of Natural Sediments in SII Mixed Gas Hydrate Formation: An Experimental Study. *Molecules* **2023**, *28*, 5887. [CrossRef] [PubMed]
204. Li, P.; Zhang, M.; Xiao, Y.; Xu, Y.; Wang, W.; Li, Y. Study on Growth and Deposition and Mechanical Properties of Hydrate in the Presence of Silty Sand. *ACS Omega* **2025**, *10*, 12334–12345. [CrossRef]
205. Gurjar, P.; Dubey, S.; Kumar, S.; Palodkar, A.V.; Kumar, A. Carbon Dioxide Sequestration as Hydrates in Clayey-Sandy Sediments: Experiments and Modeling Approach. *Chem. Eng. J.* **2023**, *475*, 146455. [CrossRef]
206. Kumar, P. Pore Scale Modelling OF $CO_2$ Sequestration. *J. Isas* **2023**, *1*, 1–14. [CrossRef]
207. Cha, M.; Hu, Y.; Sum, A.K. Methane Hydrate Phase Equilibria for Systems Containing NaCl, KCl, and $NH_4Cl$. *Fluid. Phase Equilib.* **2016**, *413*, 2–9. [CrossRef]
208. Dholabhai, P.D.; Kalogerakis, N.; Bishnoi, P.R. Equilibrium Conditions for Carbon Dioxide Hydrate Formation in Aqueous Electrolyte Solutions. *J. Chem. Eng. Data* **1993**, *38*, 650–654. [CrossRef]
209. Babu, P.; Nambiar, A.; He, T.; Karimi, I.A.; Lee, J.D.; Englezos, P.; Linga, P. A Review of Clathrate Hydrate Based Desalination to Strengthen Energy-Water Nexus. *ACS Sustain. Chem. Eng.* **2018**, *6*, 8093–8107. [CrossRef]
210. Ho-Van, S.; Bouillot, B.; Douzet, J.; Babakhani, S.M.; Herri, J.M. Cyclopentane Hydrates—A Candidate for Desalination? *J. Environ. Chem. Eng.* **2019**, *7*, 103359. [CrossRef]
211. Yan, K.F.; Zhao, J.Y.; Chen, H.; Li, X.-S.; Xu, C.G.; Chen, Z.Y.; Zhang, Y.; Wang, Y.; Feng, J.C.; Yu, Y.S. Exploring Hydration Mechanism of Salt Ions on the Methane Hydrate Formation: Insights from Experiments, QM Calculations and MD Simulations. *Chem. Eng. Sci.* **2023**, *276*, 118829. [CrossRef]
212. Madygulov, M.S.; Vlasov, V.A. Kinetics of Methane Hydrate Formation from Stirred Aqueous NaCl Solutions. *Chem. Eng. Res. Des.* **2024**, *202*, 267–271. [CrossRef]
213. Shen, S.; Wang, L.; Ge, Y.; Chu, J.; Liang, H. The Effect of Salinity on the Strength Behavior of Hydrate-Bearing Sands. *J. Mar. Sci. Eng.* **2023**, *11*, 1350. [CrossRef]
214. Queimada, A.J.; Zhang, X.; Pedrosa, N.; Salimi, B. Effect of Salts, Impurities, and Low Water Contents in the Formation of Gas Hydrates in $CO_2$-Rich Streams. *J. Chem. Eng. Data* **2024**, *69*, 3295. [CrossRef]

215. Penru, Y.; Simon, F.X.; Guastalli, A.R.; Esplugas, S.; Llorens, J.; Baig, S. Characterization of Natural Organic Matter from Mediterranean Coastal Seawater. *J. Water Supply Res. Technol.-Aqua* **2013**, *62*, 42–51. [CrossRef]
216. Rao, T.P.; Metilda, P.; Gladis, J.M. Analytical Methodologies for the Determination of Organics in Sea Water: A Review of Methods During the Last Decade and Future Scenario. *Rev. Anal. Chem.* **2006**, *25*, 11–48. [CrossRef]
217. Dittmar, T.; Koch, B.; Hertkorn, N.; Kattner, G. A Simple and Efficient Method for the Solid-Phase Extraction of Dissolved Organic Matter (SPE-DOM) from Seawater. *Limnol. Ocean. Methods* **2008**, *6*, 230–235. [CrossRef]
218. Liu, Y.; Zhang, L.; Yang, L.; Dong, H.; Zhao, J.; Song, Y. Behaviors of $CO_2$ Hydrate Formation in the Presence of Acid-Dissolvable Organic Matters. *Environ. Sci. Technol.* **2021**, *55*, 6206–6213. [CrossRef]
219. Lamorena, R.B.; Kyung, D.; Lee, W. Effect of Organic Matters on $CO_2$ Hydrate Formation in Ulleung Basin Sediment Suspensions. *Environ. Sci. Technol.* **2011**, *45*, 6196–6203. [CrossRef] [PubMed]
220. Kelleher, B.P.; Simpson, A.J.; Rogers, R.E.; Dearman, J.; Kingery, W.L. Effects of Natural Organic Matter from Sediments on the Growth of Marine Gas Hydrates. *Mar. Chem.* **2007**, *103*, 237–249. [CrossRef]
221. Park, T.; Kyung, D.; Lee, W. Effect of Organic Matter on $CO_2$ Hydrate Phase Equilibrium in Phyllosilicate Suspensions. *Environ. Sci. Technol.* **2014**, *48*, 6597–6603. [CrossRef]
222. Gainullin, S.E.; Farhadian, A.; Kazakova, P.Y.; Semenov, M.E.; Chirkova, Y.F.; Heydari, A.; Pavelyev, R.S.; Varfolomeev, M.A. Novel Amino Acid Derivatives for Efficient Methane Solidification Storage via Clathrate Hydrates without Foam Formation. *Energy Fuels* **2023**, *37*, 3208–3217. [CrossRef]
223. Bradford Vickery, H. The History of the Discovery of the Amino Acids II. A Review of Amino Acids Described Since 1931 as Components of Native Proteins. *Adv. Protein Chem.* **1972**, *26*, 81–171. [CrossRef]
224. Bavoh, C.B.; Lal, B.; Osei, H.; Sabil, K.M.; Mukhtar, H. A Review on the Role of Amino Acids in Gas Hydrate Inhibition, $CO_2$ Capture and Sequestration, and Natural Gas Storage. *J. Nat. Gas. Sci. Eng.* **2019**, *64*, 52–71. [CrossRef]
225. Li, B.; Lu, Y.-Y.; Li, Y.-L.A.; Kontakiotis, G.; Li, B.; Lu, Y.-Y.; Li, Y.-L. A Review of Natural Gas Hydrate Formation with Amino Acids. *J. Mar. Sci. Eng.* **2022**, *10*, 1134. [CrossRef]
226. Liu, Y.; Chen, B.; Chen, Y.; Zhang, S.; Guo, W.; Cai, Y.; Tan, B.; Wang, W. Methane Storage in a Hydrated Form as Promoted by Leucines for Possible Application to Natural Gas Transportation and Storage. *Energy Technol.* **2015**, *3*, 815–819. [CrossRef]
227. Cai, Y.; Chen, Y.; Li, Q.; Li, L.; Huang, H.; Wang, S.; Wang, W. $CO_2$ Hydrate Formation Promoted by a Natural Amino Acid L-Methionine for Possible Application to $CO_2$ Capture and Storage. *Energy Technol.* **2017**, *5*, 1195–1199. [CrossRef]
228. Veluswamy, H.P.; Lee, P.Y.; Premasinghe, K.; Linga, P. Effect of Biofriendly Amino Acids on the Kinetics of Methane Hydrate Formation and Dissociation. *Ind. Eng. Chem. Res.* **2017**, *56*, 6145–6154. [CrossRef]
229. Bhattacharjee, G.; Choudhary, N.; Kumar, A.; Chakrabarty, S.; Kumar, R. Effect of the Amino Acid L-Histidine on Methane Hydrate Growth Kinetics. *J. Nat. Gas. Sci. Eng.* **2016**, *35*, 1453–1462. [CrossRef]
230. Roosta, H.; Dashti, A.; Mazloumi, S.H.; Varaminian, F. Inhibition Properties of New Amino Acids for Prevention of Hydrate Formation in Carbon Dioxide–Water System: Experimental and Modeling Investigations. *J. Mol. Liq.* **2016**, *215*, 656–663. [CrossRef]
231. Sa, J.H.; Kwak, G.H.; Lee, B.R.; Park, D.H.; Han, K.; Lee, K.H. Hydrophobic Amino Acids as a New Class of Kinetic Inhibitors for Gas Hydrate Formation. *Sci. Rep.* **2013**, *3*, 2428. [CrossRef]
232. Sa, J.H.; Lee, B.R.; Park, D.H.; Han, K.; Chun, H.D.; Lee, K.H. Amino Acids as Natural Inhibitors for Hydrate Formation in $CO_2$ Sequestration. *Environ. Sci. Technol.* **2011**, *45*, 5885–5891. [CrossRef]
233. Sa, J.H.; Kwak, G.H.; Han, K.; Ahn, D.; Lee, K.H. Gas Hydrate Inhibition by Perturbation of Liquid Water Structure. *Sci. Rep.* **2015**, *5*, 11526. [CrossRef] [PubMed]
234. Li, Y.; Yin, Z.; Lu, H.; Xu, C.; Liu, X.; Huang, H.; Chen, D.; Linga, P. Evaluation of Amino Acid L-Leucine as a Kinetic Promoter for $CO_2$ Sequestration as Hydrate: A Kinetic and Morphological Study. *J. Environ. Chem. Eng.* **2023**, *11*, 111363. [CrossRef]
235. Yodpetch, V.; Inkong, K.; Veluswamy, H.P.; Kulprathipanja, S.; Rangsunvigit, P.; Linga, P. Investigation on the Amino Acid-Assisted $CO_2$ Hydrates: A Promising Step Toward Hydrate-Based Decarbonization. *ACS Sustain. Chem. Eng.* **2023**, *11*, 2797–2809. [CrossRef]
236. Srivastava, S.; Kollemparembil, A.M.; Zettel, V.; Claßen, T.; Gatternig, B.; Delgado, A.; Hitzmann, B. Experimental Investigation of $CO_2$ Uptake in $CO_2$ Hydrates Formation with Amino Acids as Kinetic Promoters and Its Dissociation at High Temperature. *Sci. Rep.* **2022**, *12*, 8359. [CrossRef]
237. Prasad, P.S.R.; Kiran, B.S. Synergistic Effects of Amino Acids in Clathrates Hydrates: Gas Capture and Storage Applications. *Chem. Eng. J. Adv.* **2020**, *3*, 100022. [CrossRef]
238. Khandelwal, H.; Qureshi, M.F.; Zheng, J.; Venkataraman, P.; Barckholtz, T.A.; Mhadeshwar, A.B.; Linga, P. Effect of l -Tryptophan in Promoting the Kinetics of Carbon Dioxide Hydrate Formation. *Energy Fuels* **2021**, *35*, 649–658. [CrossRef]
239. Liu, Z.; Zeng, Y.; Wang, W. $CO_2$ Hydrate Formation Promoted by a Bio-Friendly Amino Acid L-Isoleucine. *IOP Conf. Ser. Earth Environ. Sci.* **2020**, *474*, 052054. [CrossRef]

240. Prasad, P.S.R.; Kiran, B.S. Are the Amino Acids Thermodynamic Inhibitors or Kinetic Promoters for Carbon Dioxide Hydrates? *J. Nat. Gas. Sci. Eng.* **2018**, *52*, 461–466. [CrossRef]
241. Prasad, P.S.R.; Sai Kiran, B. Clathrate Hydrates of Greenhouse Gases in the Presence of Natural Amino Acids: Storage, Transportation and Separation Applications. *Sci. Rep.* **2018**, *8*, 8560. [CrossRef]
242. Biro, J.C. Amino Acid Size, Charge, Hydropathy Indices and Matrices for Protein Structure Analysis. *Theor. Biol. Med. Model.* **2006**, *3*, 15. [CrossRef] [PubMed]
243. Hubberten, U.; Lara, R.J.; Kattner, G. Amino Acid Composition of Seawater and Dissolved Humic Substances in the Greenland Sea. *Mar. Chem.* **1994**, *45*, 121–128. [CrossRef]
244. Bogue, D.C.; Hamilton, P.B.; Anderson, R.A. Ion Exchange Chromatography of Amino Acids Analysis of Diffusion (Mass Transfer) Mechanisms. *Anal. Chem.* **1960**, *32*, 1782–1792. [CrossRef]
245. Riley, J.P.; Segar, D.A. The Seasonal Variation of the Free and Combined Dissolved Amino Acids in the Irish Sea. *J. Mar. Biol. Assoc. U. K.* **1970**, *50*, 713–720. [CrossRef]
246. Bohling, H. Untersuchungen Über Freie Gelöste Aminosäuren in Meerwasser. *Mar. Biol.* **1970**, *6*, 213–225. [CrossRef]
247. Bohling, H. Gelöste Aminosäuren in Oberflächenwasser der Nordsee Bei Helgoland: Konzentrationsveränderungen Im Sommer 1970. *Mar. Biol.* **1972**, *16*, 281–289. [CrossRef]
248. Dawson, R.; Gary, P. The determination of α-amino acids in seawater using a fluorimetric analyser. *Mar. Chem.* **1976**, *6*, 27–40. [CrossRef]
249. Litchfield, C.D.; Prescott, J.M. Analysis by Dansylation of Amino Acids Dissolved in Marine and Freshwaters1. *Limnol. Oceanogr.* **1970**, *15*, 250–256. [CrossRef]
250. Mopper, K.; Dawson, R. Determination of Amino Acids in Sea Water-Recent Chromatographic Developments and Future Directions. *Sci. Total Environ.* **1986**, *49*, 115–131. [CrossRef]
251. Zhou, Y.; Yoon, J. Recent Progress in Fluorescent and Colorimetric Chemosensors for Detection of Amino Acids. *Chem. Soc. Rev.* **2012**, *41*, 52–67. [CrossRef]
252. Daraboina, N.; Ripmeester, J.; Walker, V.K.; Englezos, P. Natural Gas Hydrate Formation and Decomposition in the Presence of Kinetic Inhibitors. 3. Structural and Compositional Changes. *Energy Fuels* **2011**, *25*, 4398–4404. [CrossRef]
253. Liu, Y.; Feng, Y.; Zhang, L.; Song, Y.; Yang, L.; Zhao, J. Effects of Protein Macromolecules and Metabolic Small Molecules on Kinetics of Methane Hydrate Formation in Marine Clay. *Chem. Eng. J.* **2021**, *412*, 128496. [CrossRef]
254. Kelland, M.A.; Zhang, Q.; Chua, P.C. A Study of Natural Proteins and Partially Hydrolyzed Derivatives as Green Kinetic Hydrate Inhibitors. *Energy Fuels* **2018**, *32*, 9349–9357. [CrossRef]
255. Jia, Y.; Zhao, Y.; Li, M.; Zhang, L.; Liu, Y.; Dong, H.; Zhao, J.; Yang, L.; Song, Y. Biodegradable Organics as a Multisystem-Compatible Low-Dose Green Kinetic Hydrate Inhibitor. *ACS Sustain. Chem. Eng.* **2022**, *10*, 11320–11329. [CrossRef]
256. Venketesh, S.; Dayananda, C. Properties, Potentials, and Prospects of Antifreeze Proteins. *Crit. Rev. Biotechnol.* **2008**, *28*, 57–82. [CrossRef] [PubMed]
257. Scholander, P.F.; van Dam, L.; Kanwisher, J.W.; Hammel, H.T.; Gordon, M.S. Supercooling and Osmoregulation in Arctic Fish. *J. Cell Comp. Physiol.* **1957**, *49*, 5–24. [CrossRef]
258. DeVries, A.L.; Wohlschlag, D.E. Freezing Resistance in Some Antarctic Fishes. *Science* **1969**, *163*, 1073–1075. [CrossRef]
259. Kristiansen, E.; Ramløv, H.; Højrup, P.; Pedersen, S.A.; Hagen, L.; Zachariassen, K.E. Structural Characteristics of a Novel Antifreeze Protein from the Longhorn Beetle Rhagium Inquisitor. *Insect Biochem. Mol. Biol.* **2011**, *41*, 109–117. [CrossRef]
260. Middleton, A.J.; Brown, A.M.; Davies, P.L.; Walker, V.K. Identification of the Ice-Binding Face of a Plant Antifreeze Protein. *FEBS Lett.* **2009**, *583*, 815–819. [CrossRef]
261. Celik, Y.; Graham, L.A.; Mok, Y.F.; Bar, M.; Davies, P.L.; Braslavsky, I. Superheating of Ice Crystals in Antifreeze Protein Solutions. *Proc. Natl. Acad. Sci. USA* **2010**, *107*, 5423–5428. [CrossRef]
262. Tomczak, M.M.; Marshall, C.B.; Gilbert, J.A.; Davies, P.L. A Facile Method for Determining Ice Recrystallization Inhibition by Antifreeze Proteins. *Biochem. Biophys. Res. Commun.* **2003**, *311*, 1041–1046. [CrossRef]
263. HEW, C.L.; YANG, D.S.C. Protein Interaction with Ice. *Eur. J. Biochem.* **1992**, *203*, 33–42. [CrossRef]
264. Nada, H.; Furukawa, Y. Antifreeze Proteins: Computer Simulation Studies on the Mechanism of Ice Growth Inhibition. *Polym. J.* **2012**, *44*, 690–698. [CrossRef]
265. Hudait, A.; Qiu, Y.; Odendahl, N.; Molinero, V. Hydrogen-Bonding and Hydrophobic Groups Contribute Equally to the Binding of Hyperactive Antifreeze and Ice-Nucleating Proteins to Ice. *J. Am. Chem. Soc.* **2019**, *141*, 7887–7898. [CrossRef]
266. Zeng, H.; Wilson, L.D.; Walker, V.K.; Ripmeester, J.A. The Inhibition of Tetrahydrofuran Clathrate-Hydrate Formation with Antifreeze Protein. *Can. J. Phys.* **2003**, *81*, 17–24. [CrossRef]
267. Sun, T.; Davies, P.L.; Walker, V.K. Structural Basis for the Inhibition of Gas Hydrates by α-Helical Antifreeze Proteins. *Biophys. J.* **2015**, *109*, 1698–1705. [CrossRef]
268. Al-Adel, S.; Dick, J.A.G.; El-Ghafari, R.; Servio, P. The Effect of Biological and Polymeric Inhibitors on Methane Gas Hydrate Growth Kinetics. *Fluid. Phase Equilib.* **2008**, *267*, 92–98. [CrossRef]

269. Scotter, A.J.; Marshall, C.B.; Graham, L.A.; Gilbert, J.A.; Garnham, C.P.; Davies, P.L. The Basis for Hyperactivity of Antifreeze Proteins. *Cryobiology* **2006**, *53*, 229–239. [CrossRef] [PubMed]
270. Zhou, H.; Infante Ferreira, C. Effect of Type-III Anti-Freeze Proteins (AFPs) on $CO_2$ Hydrate Formation Rate. *Chem. Eng. Sci.* **2017**, *167*, 42–53. [CrossRef]
271. Zhang, Y.; Yuan, C.; Chen, Z.; Chen, C.; Liang, X.; von Solms, N.; Song, Y. Molecular Insights into the Synergistic Inhibition Mechanisms of Antifreeze Protein and Methanol on Carbon Dioxide Hydrate Growth. *Energy* **2024**, *310*, 133239. [CrossRef]
272. Lowry, O.H.; Rosebrough, N.J.; Farr, A.L.; Randall, R.J. Protein measurement with the Folin phenol reagent. *J. Biol. Chem.* **1951**, *193*, 265–275. [CrossRef] [PubMed]
273. Crompton, T.R. *Analysis of Seawater A Guide for the Analytical and Environmental Chemist*; Springer: Berlin/Heidelberg, Germany, 2006. [CrossRef]
274. Packard, T.T.; Dortch, Q. Particulate Protein-Nitrogen in North Atlantic Surface Waters. *Mar. Biol.* **1975**, *33*, 347–354. [CrossRef]
275. Tanoue, E. Detection of Dissolved Protein Molecules in Oceanic Waters. *Mar. Chem.* **1995**, *51*, 239–252. [CrossRef]
276. Sutton, R.; Sposito, G. Molecular Structure in Soil Humic Substances: The New View. *Environ. Sci. Technol.* **2005**, *39*, 9009–9015. [CrossRef] [PubMed]
277. Lv, T.; Pan, J.; Chen, Z.; Cai, J.; Li, X.; Zhang, Y. Kinetic Study of Fulvic Acid on Methane Hydrate Formation and Decomposition in Clay-Rich Silty Sediments. *J. Pet. Sci. Eng.* **2022**, *217*, 110916. [CrossRef]
278. Kononova, M.M. *Soil Organic Matter, Its Nature, Its Role in Soil Formation and in Soil Fertility*, 2nd ed.; Pergamon Press Ltd.: Oxford, UK, 1966.
279. Lv, T.; Li, X.; Chen, Z.; Yan, K.; Zhang, Y. Effect of Fulvic Acid on Methane Hydrate Formation and Dissociation in Mixed Porous Media. *Energy Procedia* **2019**, *158*, 5323–5328. [CrossRef]
280. Ji, H.; Wu, G.; Zi, M.; Chen, D. Microsecond Molecular Dynamics Simulation of Methane Hydrate Formation in Humic-Acid-Amended Sodium Montmorillonite. *Energy Fuels* **2016**, *30*, 7206–7213. [CrossRef]
281. Strukov, D.; Sagidullin, A.; Kartopol'cev, S.; Rodionova, T.; Manakov, A. Investigation of the Kinetic Promoting Effect of Humic Acids on the Formation of Methane Hydrate. *Chem. Eng. Sci.* **2025**, *309*, 121477. [CrossRef]
282. Liu, F.; Wang, Y.; Lang, X.; Li, G.; Fan, S. Rapid Formation of $CO_2$ Hydrate with High Storage Capacity via a Novel "Self-Siphoning" Principle. *Chem. Eng. J.* **2025**, *513*, 162749. [CrossRef]
283. Aro, T.; Fatehi, P. Production and Application of Lignosulfonates and Sulfonated Lignin. *ChemSusChem* **2017**, *10*, 1861–1877. [CrossRef]
284. Yi, J.; Zhong, D.L.; Yan, J.; Lu, Y.Y. Impacts of the Surfactant Sulfonated Lignin on Hydrate Based $CO_2$ Capture from a $CO_2/CH_4$ Gas Mixture. *Energy* **2019**, *171*, 61–68. [CrossRef]
285. Huang, H.; Liu, X.; Lu, H.; Xu, C.; Zhao, J.; Li, Y.; Gu, Y.; Yin, Z. Introducing Sodium Lignosulfonate as an Effective Promoter for $CO_2$ Sequestration as Hydrates Targeting Gaseous and Liquid $CO_2$. *Adv. Appl. Energy* **2024**, *14*, 100175. [CrossRef]
286. Qiu, X.; Kong, Q.; Zhou, M.; Yang, D. Aggregation Behavior of Sodium Lignosulfonate in Water Solution. *J. Phys. Chem. B* **2010**, *114*, 15857–15861. [CrossRef]
287. Othman, N.; Ooi, Z.Y.; Harruddin, N. Selection of liquid membrane component for lignosulfonate removal from liquid waste solution using emulsion liquid membrane process. *J. Appl. Membr. Sci. Technol.* **2017**, *14*. [CrossRef]
288. Pocklington, R.; Hardstaff, W.R. Rapid Semiquantitative Screening Procedure for Lignin in Marine Sediments. *J. Int. Conf. Explor. Sea* **1974**, *36*, 92–94. [CrossRef]
289. Louchouam, P.; Opsahl, S.; Benner, R. Isolation and Quantification of Dissolved Lignin from Natural Waters Using Solid-Phase Extraction and GC/MS. *Anal. Chem.* **2000**, *72*, 2780–2787. [CrossRef]
290. Hedges, J.I.; Ertel, J.R. Characterization of Lignin by Gas Capillary Chromatography of Cupric Oxide Oxidation Products. *Anal. Chem.* **1982**, *54*, 174–178. [CrossRef]
291. Rupp, E.; Zuman, P. The Use of Differential Pulse and D.C. Polarography in the Analysis of Solutions Containing Surfactants. *Anal. Lett.* **1994**, *27*, 939–955. [CrossRef]
292. Almgren, T.; Josefsson, B.; Nyquist, G. A Fluorescence Method for Studies of Spent Sulfite Liquor and Humic Substances in Sea Water. *Anal. Chim. Acta* **1975**, *78*, 411–422. [CrossRef]
293. King, L.H. *Isolation and Characterization of Organic Matter from Glacial-Marine Sediments on the Scotian Shelf*; Bedford Institute of Oceanography: Bedford, UK, 1967; pp. 1–16.
294. Pierce, R.H., Jr.; Felbeck, G.T., Jr. A Comparison of Three Methods of Extracting Organic Matter from Soils and Marine Sediments. In Proceedings of the International Meeting of Humic Substances, Nieuwersluis, The Netherlands, 29–31 May 1972.
295. Rashid, M.A.; King, L.H. Molecular Weight Distribution Measurements on Humic and Fulvic Acid Fractions from Marine Clays on the Scotian Shelf. *Geochim. Cosmochim. Acta* **1969**, *33*, 147–151. [CrossRef]
296. Seeberg-Elverfeldt, J.; Schlüter, M.; Feseker, T.; Kölling, M. Rhizon Sampling of Porewaters near the Sediment-Water Interface of Aquatic Systems. *Limnol. Oceanogr. Methods* **2005**, *3*, 361–371. [CrossRef]

297. Shaw, T.J. An Apparatus for Fine-Scale Sampling of Pore Waters and Solids in High Porosity Sediments: Research Method Paper. *J. Sediment. Res.* **1989**, *59*, 633–634. [CrossRef]
298. Moncur, M.C.; Blowes, D.W.; Ptacek, C.J. Pore-Water Extraction from the Unsaturated and Saturated Zones. *Can. J. Earth Sci.* **2013**, *50*, 1051–1058. [CrossRef]
299. de Lange, G.J. Shipboard Routine and Pressure-Filtration System for Pore-Water Extraction from Suboxic Sediments. *Mar. Geol.* **1992**, *109*, 77–81. [CrossRef]
300. Wang, Y.; Guo, J.; Tan, X.; Chen, J.; Fang, Y.; Wang, W.; Ge, Y. Pore Water Pressure Maintaining Sampler for Deployment on Deep-Sea ROV-Jellyfish. *Deep Sea Res. Part I Oceanogr. Res. Pap.* **2024**, *203*, 104194. [CrossRef]
301. Falter, J.L.; Sansone, F.J. Shallow Pore Water Sampling in Reef Sediments. *Coral Reefs* **2000**, *19*, 93–97. [CrossRef]
302. Mantoura, R.F.C.; Riley, J.P. The Analytical Concentration of Humic Substances from Natural Waters. *Anal. Chim. Acta* **1975**, *76*, 97–106. [CrossRef]
303. Schnitzer, M. Chemical, Spectroscopic, and Thermal Methods for the Classification and Characterization of Humic Substances. In Proceedings of the International Meeting of Humic Substances, Nieuwersluis, The Netherlands, 29–31 May 1972.
304. Manka, J.; Rebhun, M.; Mandelbaum, A.; Bortinger, A. Characterization of Organics in Secondary Effluents. *Environ. Sci. Technol.* **1974**, *8*, 1017–1020. [CrossRef]
305. Skinner, S.I.M.; Schnitzer, M. Rapid Identification by Gas Chromatography-Mass Spectrometry-Computer of Organic Compounds Resulting from the Degradation of Humic Substances. *Anal. Chim. Acta* **1975**, *75*, 207–211. [CrossRef]
306. Schnitzer, M.; Stewart, D.; Skinner, I.M. The Low Temperature Oxidation of Humic Substances. *Can. J. Chem.* **1974**, *52*, 1072–1080. [CrossRef]